Published in final edited form as:

Nature. 2014 April 3; 508(7494): 123–127. doi:10.1038/nature13158.

Maternal retinoids control type 3 innate lymphoid cells and set the offspring immunity

Serge A. van de Pavert[*,1,†], **Manuela Ferreira**[*,2], **Rita G. Domingues**[2], **Hélder Ribeiro**[2], **Rosalie Molenaar**[1], **Lara Moreira-Santos**[2], **Francisca F. Almeida**[2], **Sales Ibiza**[2], **Inês Barbosa**[2], **Gera Goverse**[1], **Carlos Labão-Almeida**[2], **Cristina Godinho-Silva**[2], **Tanja Konijn**[1], **Dennis Schooneman**[1], **Tom O'Toole**[1], **Mark R. Mizee**[1], **Yasmin Habani**[1], **Esther Haak**[3], **Fabio R. Santori**[4], **Dan R. Littman**[4], **Stefan Schulte-Merker**[5], **Elaine Dzierzak**[3], **J. Pedro Simas**[2], **Reina E. Mebius**[*,1], and **Henrique Veiga-Fernandes**[*,2]

[1]Department of Molecular Cell Biology and Immunology, VU University Medical Center, Amsterdam, Netherlands [2]Instituto de Medicina Molecular, Faculdade de Medicina de Lisboa, Av. Prof. Egas Moniz, Edifício Egas Moniz, 1649-028 Lisboa, Portugal [3]Department of Cell Biology, Erasmus Medical Center, Rotterdam, Netherlands [4]Howard Hughes Medical Institute, Molecular Pathogenesis Program, Skirball Institute of Biomolecular Medicine, New York University School of Medicine, New York, USA [5]Hubrecht Institute–KNAW (Royal Netherlands Academy of Arts and Sciences) and University Medical Center Utrecht, 3584 CT Utrecht, Netherlands

Abstract

The impact of the nutritional status during foetal life in the overall health of adults has been recognised[1]. However dietary effects on the developing immune system are largely unknown. Development of secondary lymphoid organs (SLOs) occurs during embryogenesis and is considered to be developmentally programmed[2,3]. SLO formation dependents on a subset of type 3 innate lymphoid cells (ILC3) named lymphoid tissue inducer (LTi) cells[2,3,4,5]. Here we show that foetal ILC3s are controlled by cell-autonomous retinoic acid (RA) signalling *in utero* pre-setting the immune fitness in adulthood. We found that embryonic lymphoid organs contain ILC progenitors that differentiate locally into mature LTi cells. Local LTi differentiation was controlled by maternal retinoid intake and foetal RA signalling acting in a haematopoietic cell-autonomous manner. RA controlled LTi cell maturation upstream of the transcription factor RORγt.

Correspondence and requests for materials should be addressed to H.V.-F. (jhfernandes@fm.ul.pt).

[†]Current address: Hubrecht Institute–KNAW (Royal Netherlands Academy of Arts and Sciences) and University Medical Center Utrecht, 3584 CT Utrecht, Netherlands.

[*]These authors contributed equally to this work

Author contribution M.F. wrote the manuscript, designed, performed and analysed the experiments in Figures: 1a,b,d,e,g,h,i; 2a,b,c,d,e,f,g,h; 3a,b,d,e,f,g,h,i; 4a,b,d,e,f,g,h,i,j; and Extended Data Figures: 1a,d,e,f; 2a,b,c,d; 3a,b,c,d,e,f,g,h; 4a,b,c,d; 5a,b,c; 6; 7a,b,c,d,e,f; 8a,b,c,d; 9a,b; 10a,b,c;. S.A.vd.P. wrote the manuscript, designed, performed and analysed the experiments in Figures: 1c,f; 3c,g,h,i; 4c; and Extended Data Figures: 1b,c,e; 5b,c; 6. R.G.D., H.R., R.M., L.M.–S., F.F.A., S.I., I.B., G.G., C.L.-A., T.K., D.S., T.O'T., M.R.M., Y.H., S.S-M. contributed to several experiments. C.G.-S. and J.P.S. provided Murid herpesvirus-4. D.R.L. and F.R.S provided *Rorgt*$^{-/-}$ embryos. E.H. and E.D. provided Ly-6A (*Sca1*)-*GFP* mice. R.E.M. and H.V.-F. supervised the work, planned the experiments and wrote the manuscript.

Author information The authors declare no competing financial interests.

Accordingly, enforced expression of *Rorgt* restored maturation of LTi cells with impaired RA signalling, while RA receptors directly regulated the *Rorc* locus. Finally, we established that maternal levels of dietary retinoids control the size of secondary lymphoid organs and the efficiency of immune responses in the adult offspring. Our results reveal a molecular link between maternal nutrients and the formation of immune structures required for resistance to infection in the offspring.

Haematopoietic cells that initially colonise SLO sites include CD3$^-$c-Kit$^+$IL7Rα$^-$α4β7$^+$CD11c$^+$CD4$^-$ Lymphoid Tissue initiator (LTin) cells and the prototypical member of type 3 ILCs, LTi cells[2,3,4,5,6,7]. While the majority of LTi cells express CD4, this is a late event in LTi differentiation and not all RORγt$^+$ LTi cells express this marker[5,6,8,9]. Thus, we hypothesised that CD3$^-$IL7Rα$^+$α4β7$^+$ID2$^+$c-Kit$^+$CD11c$^-$CD4$^-$ ILCs (herein called ILC$_{4neg}$ cells) receive local cues giving rise to ID2$^+$RORγt$^+$CD4$^+$ LTi cells (LTi$_4$) within developing SLOs. Noteworthy, enteric ILC$_{4neg}$ cells include mainly ID2$^+$RORγt$^+$CD4$^-$ LTi cells (LTi$_0$) but also a small fraction of ID2$^+$RORγt$^-$CD4$^-$ precursors with LTi cell potential (herein called pre-ILC cells)[9]. In contrast, nearly 100% of LN ILC$_{4neg}$ cells are LTi$_0$ cells (Extended Data Fig. 1a,b). Analysis of E12.5 guts revealed that ILC$_{4neg}$ cells are the only appreciable IL7Rα$^+$ colonising cells (Fig. 1a,b). Accordingly, non-cycling mature Sca1$^-$ LTi$_4$ cells increased throughout development, seemingly at the expense of Sca1$^+$ ILC$_{4neg}$ cells (Fig. 1a–c; Extended Data Fig. 1c). Further evidence that ILC$_{4neg}$ cells differentiate locally was provided by organ cultures and transplantation of E12.5 intestines. Despite absence of foetal liver out-put in these settings, LTi$_4$ cells increased with time at the expense of local ILC$_{4neg}$ cells (Fig. 1d,e). Furthermore, in E14.5 *Rorgt*$^{-/-}$ embryos ILC$_{4neg}$ cells were attracted to the intestine and LNs, supporting initial anlagen colonisation by these cells (Extended Data Fig. 1d,e). Strikingly, RA stimulation of E13.5 LN cells showed increased frequency of LTi$_4$ cells and reduction of ILC$_{4neg}$ cells suggesting that differentiation of LTi$_4$ cells is regulated by RA (Fig. 1f). To confirm the effect of RA in LTi differentiation *in vivo*, pregnant mice received RA enriched diet starting at E10.5. Supplementation of RA increased LTi$_4$ cells in the embryo, in detriment of ILC$_{4neg}$ cells (Fig. 1f). In agreement, provision of the RA signalling inhibitor BMS493 to pregnant females resulted in decrease of foetal LTi$_4$ cells despite normal frequency of foetal liver progenitors and enteric haematopoietic cells (Fig. 1f; Extended Data Fig. 1f). Consequently, despite normal embryo size BMS493 administration led to reduction in LN dimensions and PP developmental failure (Fig.1g–i; Extended Data Fig.1g). Collectively, our data indicate that maternal retinoids control LTi cell differentiation within developing SLOs.

RA is a vitamin A metabolite that controls early vertebrate development, some immune processes in adulthood and it was shown to mediate CXCL13 expression in foetal mesenchymal cells[10,11,12,13,14,15,16]. RA binds to heterodimers formed by the RA receptors (RARs) and retinoid X receptors (RXRs), which bind DNA RA response elements (RAREs)[11]. In order to address putative RA cell-autonomous responses, we assessed RAR and RXR expression in E15.5 ILC$_{4neg}$, LTi$_4$ and LTin cells. RARs and RXRs were predominantly expressed by ILC$_{4neg}$ and LTi$_4$ cells, while LTin cells expressed these molecules at lower levels (Fig.2a). RA stimulation revealed that only ILC$_{4neg}$ and LTi$_4$ cells respond robustly as shown by *Rarb* up-regulation (Fig.2b)[16]. Altogether, these data suggest

that impaired SLO development in BMS493 treated mice might be the consequence of RA signal ablation in LTi cells. To test this hypothesis we employed a lineage-targeted model to block RA signalling. We used a mouse line in which a truncated form of the RARα gene was knocked into the *ROSA26* locus preceded by a triple polyadenylation signal flanked by two loxP sites (*ROSA26*-RARα403). This line was bred to *Vav*-iCre mice that in contrast to other tested Cre lines ensured Cre activity in foetal LTin, ILC_{4neg} and LTi_4 cells (Extended Data Fig.2a–d)[17,18]. Despite normal frequencies of foetal liver precursors, and SLO LTin, ILC_{4neg} and LTi_0 cells, *Vav*-iCre/*ROSA26*-RARα403 embryos (Rar mice) revealed a dose-dependent reduction of LTi_4 cells (Fig.2c,d; Extended Data Fig.3a–f). To assess whether the differentiation potential of ILC_{4neg} cells is controlled by RA thresholds, we cultured purified ILC_{4neg} cells from Rar^{Het}, Rar^{Hom} and WT littermate control mice. While WT ILC_{4neg} cells upregulated pro-inflammatory cytokines and chemokines and gave rise to LTi_4 cells in vitro, these were impaired proportionally to the degree of RA signalling abrogation in ILC_{4neg} cells (Fig.2e,f; Extended Data Fig.3g). Finally, despite normal frequency of colonising ILC_{4neg} cells (Fig.2d), haematopoietic cell-autonomous impairment of RA responses resulted in severely diminished foetal LN size and reduced number of minute PPs (Fig.2g,h; Extended Data Fig.3h). Altogether our data indicate that LTi cell differentiation is controlled by cell-autonomous RA signalling in developing SLOs.

Previous reports have identified key LTi cell regulators[2]. Mice mutant for the transcription factors ID2 and RORγt lack LTi cells and do not develop SLOs[19,20]. *Runx1*, *Tox* and *Notch1* were also implicated in LTi cell maturation[9,21,22,23]. We found that while most LTi related genes were normally expressed in Rar^{Hom} and Rar^{Het} ILC_{4neg} and LTi_4 cells, *Runx1* was increased and *Rorgt* was reduced (Fig.3a; Extended Data Fig.4a–d). Expression of pro-inflammatory genes was also reduced in Rar^{Hom} and Rar^{Het} ILC_{4neg} and LTi_4 cells (Fig.3a; Extended Data Fig.4b–d). The marked reduction of *Rorgt* suggested that RA could provide ILC_{4neg} cells with signals leading to *Rorgt* regulation. Accordingly, RA stimulation of ILC_{4neg} cells resulted in *Rorgt* up-regulation while most other transcription factors were unperturbed, notably *Runx1* (Fig.3b). In agreement, BMS493 inhibited RA induced *Rorgt* and efficient block of RORγt by digoxin prevented RA induced differentiation of ILC_{4neg} cells into LTi_4 cells, while cell viability was unaffected (Fig.3c; Extended Data Fig.5a–c). To further test whether RA induced LTi maturation required RORγt, we determined if differentiation of RAR dominant negative ILC_{4neg} cells was restored by enforced *Rorgt* expression. Retro-viral transduction of *Rorgt* revealed that RAR dominant negative ILC_{4neg} cells restored high levels of pro-inflammatory genes and reacquired their potential to differentiate towards LTi_4 cells (Fig.3d–f). Further evidence that RA can directly regulate *Rorgt* expression was provided by computational analysis of potential RARE sites and chromatin immuno precipitation (ChIP) with pan-RAR and RXR antibodies. RA stimulation resulted in increased binding of RAR and RXR upstream and within the *Rorc* gene (Fig. 3g,h; Extended Table 1). To analyse the role of these sites we introduced the RARE C (−5,478 *Rorg* TSS), E (−1,800 *Rorg* TSS) and G (−1,619 *Rorgt* TSS) half-sites in a Luciferase reporter vector. Mutations in these sites resulted in significant reduction of the regulatory function of these elements as measured by Luciferase activity (Fig.3i). Thus, cell-autonomous RA signalling provides LTi cells with critical differentiation signals via direct regulation of *Rorgt*.

Our data suggest that mature LTi cell numbers regulate the size of SLO primordia and may determine lymphoid organ size in adulthood[24]. Rar^{Het} adult mice revealed reduced SLOs and lymphocyte numbers when compared to their WT littermate controls (Fig.4a,b; Extended Data Fig.6a,b). In agreement, mice that received vitamin A deficient (VAD) diet throughout life had reduced lymphoid organ size when compared to vitamin A control mice (VAC) (Fig.4c). However, since Rar^{Het} and VAD lymphocytes have life-long access to altered levels of RA signals, it is possible that SLO size might be a consequence of altered lymphocyte pools[12,13,14,15]. To clarify this issue, we provided pregnant mice with vitamin A high (VAH), VAD or VAC diet and switched all diets to the same VAC diet after birth. At 10 weeks of age mice that were exposed to VAH diet exclusively *in utero* had larger SLOs while VAD diet exposed mice had small SLOs when compared to VAC control mice (Fig. 4d). Interestingly, provision of variable vitamin A diet levels exclusively after birth no longer controlled SLO size (Extended Data Fig.6c,d). Additional evidence that RA determines SLO size in early life was provided by transplantation of CD45.1 WT bone marrow into lethally irradiated Rar^{Het} ($WT \rightarrow Rar^{Het}$) or WT ($WT \rightarrow WT$) CD45.2 littermate control hosts at 2 weeks of age (Fig.4e). Thus, we generated mice that pre- and peri-natally received low input of RA signals in haematopoietic cells, but that upon transplantation harbour a normal WT haematopoietic system. $WT \rightarrow Rar^{Het}$ mice, which received low RA cues *in utero*, exhibited small SLOs when compared to their $WT \rightarrow WT$ counterparts at 8 weeks after transplantation (Fig.4f,g; Extended Data Fig.6e,f). This phenotype also revealed reduced lymphocyte numbers, albeit normal SLO organisation and similar haematopoietic cell reconstitution (Fig.4h; Extended Data Fig.6f; Extended Data Fig.7a–d). In agreement, dendritic cells from $WT \rightarrow Rar^{Het}$ or $WT \rightarrow WT$ chimeras had similar capacity to activate lymphocytes (Extended Data Fig. 7e,f).

Our data suggest that available RA *in utero* regulates the size of lymphocyte pools in the offspring, with possible consequences on their adaptive immune responses. To test this hypothesis, $WT \rightarrow Rar^{Het}$ or $WT \rightarrow WT$ chimeras were infected intranasally with Murid herpesvirus-4, resulting in acute lung infection. Analysis of draining intrathoracic LNs revealed reduced expansion but normal frequency of $CD8^+$ T cells specific for the viral epitopes ORF61 and ORF75c in $WT \rightarrow Rar^{Het}$ mice (Fig.4i; Extended Data Fig.8a–c). Consequently, while $WT \rightarrow WT$ chimeras efficiently cleared lytic virus by day 10, high viral titres were still detected in $WT \rightarrow Rar^{Het}$ chimeras 14 days after infection (Fig.4j)[25]. Thus, a deficit of RA signals within haematopoietic cells in early life results in small SLOs and poor capacity to control infection.

Defining the requirements that control SLO development is essential to understand how immunity may be regulated. We now show that RA controls LTi cells, regulating LTi pro-inflammatory genes and the frequency of LTi_4 cells (Extended Data Fig.9). RA operates in a cell-autonomous fashion, via RORγt, although additional factors regulate *Rorgt* in ILC3s.

SLO development has been considered to be developmentally programmed; we now show that formation of these structures can be also controlled by dietary signals. Thus, in addition to the established impact of dietary plant-derived chemicals in post-natal immune cells, our work reveals dietary retinoids as key regulators of pre-natal ILCs with a lifelong impact in adult lymphoid organ size[26,27,28]. It was previously shown that complete absence of

lymphoid organs leads to long-life virus persistence[29]. Our data reveal that the efficiency of adaptive immune responses to infection and possibly to other immune insults may be pre-tuned in early life through dietary signals from maternal origin.

We report here that cell-autonomous RA signalling is a key axis for *Rorgt* expression and LTi cell differentiation within developing SLOs. Similarly, RA may also be important after birth in infection and chronic inflammatory diseases[30]. Lineage targeted strategies will be central to elucidate the contribution of dietary retinoids in these outcomes.

Methods Summary

Mice were maintained at IMM or VU University Medical Centre according to national and international guidelines. Bone marrow cells were isolated from 8 week-old C57Bl/6 CD45.1 mice and injected intravenously into 2 week-old lethally irradiated CD45.2 *ROSA26*-RARa403^{Het} (WT→Rar^{Het}) or WT littermate controls (WT→WT). C57Bl/6 female mice received either vitamin A deficient (VAD), with no vitamin A (vitamin free casein), vitamin A high (VAH, 25,000IU/Kg) or vitamin A control (VAC, 4,000IU/kg) diets. Retinoic acid was provided to pregnant mice from E10.5 until sacrifice. Quantitative real time RT-PCR was performed as previously described[6,7,10]. Computational analysis was performed with TESS. DNA/protein complexes were immunoprecipitated using antibodies against mouse pan-RAR, pan-RXR or control IgG.

Methods

Mice

C57Bl/6 mice were purchased from Charles River and C57Bl/6 CD45.1 mice were obtained at IMM. *Vav-iCre*[17], *hCD2-GFP*[6], *Id2-CreERT2*[31], *ROSA26-RARa403*[18], *Rorgt-Cre*[32], *ROSA26-eYFP*[33], *hCD2-Cre*[17], *ROSA26-mGFPTomato*[34], Ly-6A (*Sca1*) *GFP*[35], *Rorgt*$^{-/-}$ [19], *Id2-GFP*[31], and *OT1* Tg *Rag1*$^{-/-}$ [36,37] mice were previously described. Tamoxifen (2mg/female) was injected daily into *Id2-CreERT2* pregnant females from E8.5 to E13.5. All animal experiments were approved by national and institutional ethical committees. Direção Geral de Veterinária and IMM ethical committee (IMM) and Animal Experimental Committee, VU University (VUMC). Power Analysis was performed in order to estimate the number of experimental mice.

Bone marrow transplantation

Bone marrow cells were isolated from 8 week-old C57Bl/6 CD45.1 mice and 5×10^6 cells were injected intravenously into 2 week-old lethally irradiated (1,000 rad) CD45.2 *ROSA26*-RARa403^{Het} (WT→Rar^{Het}) or CD45.2 WT littermate controls (WT→WT).

Vitamin A Diets

C57Bl/6 female mice received either vitamin A deficient (VAD), with no vitamin A (vitamin free casein), vitamin A high (VAH, 25,000IU/Kg) or vitamin A control (VAC, 4,000IU/kg) diet at E8.5 or 2 weeks before coitus in Fig.4d. Diets were purchased from MP Biomedical (AIN93M feed, Solon, Ohio, USA) (please see also below). RA is rapidly degraded under

normal light and temperature conditions; thus it is unlikely that bioactive RA is present in normal diets. Therefore, bioactive RA levels in the differently used diets or normal chow is negligible. Analysis of the adult offspring with life-long diet (mice kept under VAD, VAH or VAC diet until analysis) was performed at 10 weeks of age. Analysis of the adult offspring with pre- and peri-natal VAH and VAD diet (*in utero*) was performed at 10 weeks of age (all mice were switched to the same VAC diet after birth). Post-birth diet experiments (VAD, VAH and VAC) were initiated at 6 weeks of age and analysed at 13 weeks of age. For adult SLO analysis axillary, brachial, inguinal and intrathoracic LNs and Peyer's patches (PPs) were carefully dissected. Dimensions were determined using a Zeiss Stereo Lumar V12 microscope with a Zeiss Neolumar S 0.8X objective and weights determined with precision scales (Sartorius). Vitamin A deficient diet had similar composition to control diet but with no added vitamin A palmitate. Vitamin A high diet contained 1g vitamin A palmitate (250,000U/g) per 10kg of diet. Thus, 10Kg of vitamin A control diet was composed of 4,657g corn starch, 1,400g vitamin free Casein, 1,550g dextrinized corn starch, 1,000g sucrose, 400g soybean oil, 500g Alphacel non-nutrive bulk, 350g AIN-93M mineral mix, 18g L-Cystine, 25g Choline Bitartrate, 0.080g T-Butyl Hydroquinone, 0.3g Niacin, 0.16g D-Calcium Pantothenate, 0.07g Pyridoxine HCl, 0.06g Thiamine HCl, 0.06g Riboflavin, 0.02g Folic acid, 0.002g Biotin, 0.25g vitamin B-12 (0.1%Trit), 3g Alpha Tocopherol powder (250U/g), 0.16g vitamin A palmitate (250,000U/g), 0.025 g vitamin D3 (400,000U/g), 0.008g Phylloquinone and 96 g powder sugar.

Retinoic acid and BMS493 treatment

For *in vivo* stimulation, retinoic acid was provided to pregnant mice as previously described[38]. In short, mice were mated overnight and the day of vaginal plug detection was marked as E0.5. Retinoic acid supplemented food was given from E10.5 until sacrifice (Sigma-Aldrich, 250mg/g chow or vehicle, i.e., ethanol). Food was stored in the dark at 4°C and refreshed every day until sacrifice. For *in vivo* blocking of retinoic acid signalling, pregnant C57BL/6 mice were treated with *in vivo* pan-RAR inverse agonist BMS493 (Tocris Bioscience) (5mg/kg) or vehicle (DMSO) 1:10 in corn oil.

Kidney capsule and *ex-vivo* differentiation assay

E12.5 intestines (CD45.2) were transplanted under the kidney capsule of anaesthetised 6 to 7 week-old C57Bl/6 CD45.1 mice. For explant organ cultures E12.5 intestines were micro dissected and cultured as previously described[6,39]. Intestines were digested with collagenase D (5mg/ml; Roche) and DNase I (0.1mg/ml; Roche) and were analysed by flow cytometry.

Confocal microscopy

Gut whole mount analysis was performed as previously described[6,39]. For embryo whole mount analysis, E15.5 mice were fixed with 4% paraformaldehyde and incubated in blocking/permeabilising buffer (PBS containing 10% foetal bovine serum, 2% BSA and 0.3% Triton X-100). Embryos were incubated at 4°C overnight with primary and secondary antibodies. Samples were cleared using benzyl-alcohol-benzyl-benzoate (BABB) and were imaged in a Zeiss LSM 710 (Carl Zeiss) using EC Plan-Neofluar 10x/0.30 M27 and objective Plan Apochromat 20x/0.8 M27. Images were processed using Zeiss LSM Image Browser 4.2 software (Carl Zeiss).

Immunofluorescence analysis of embryo sections were performed as previously described[10]. Briefly, samples were formalin fixed and 8μm cryosections were dehydrated in acetone for 10 minutes. Sections were air-dried for 10 minutes. Cryosections were post-fixed 30 minutes with 1% formalin, pre-incubated for 1 hour with PBS containing 10% normal goat serum and 0.2% Triton X-100. Sections were incubated 90 minutes with primary and secondary antibodies in PBS containing 0.2% Triton X-100 and 2% normal goat serum. Sections were embedded in Mowiol with DAPI (Calbiochem) and analysed using Leica SP2 confocal laser scanning microscope.

For immunofluorescence analysis of adult lymph nodes, samples were snap frozen in isopenthane pre-cooled in liquid nitrogen and kept at −80°C. Lymph nodes were sectioned (5μm sections), fixed with 4% paraformaldehyde for 10 minutes and incubated in blocking/permeabilising buffer (PBS containing 10% fetal bovine serum, 2% BSA and 0.3% Triton X-100). Samples were incubated with primary and secondary antibodies overnight or for 2 hours in PBS containing 10% foetal bovine serum, 2% BSA and 0.3% Triton X-100. Sections were mounted in Mowiol with DAPI (Calbiochem). Images were acquired on Zeiss LSM 710 (Carl Zeiss) using EC Plan-Neofluar 10x/0.30 M27 and objective Plan Apochromat 20x/0.8 M27. Images were processed using Zeiss LSM Image Browser 4.2 software (Carl Zeiss).

Flow cytometry analysis and cell sorting

Embryonic guts and lymph nodes were harvested, digested with collagenase D (5mg/ml; Roche) or Blenzyme 2 (0.5mg/ml, Roche) and DNase I (0.1mg/ml; Roche) in DMEM, 3% FBS for approximately 40 minutes at 37°C under gentle agitation. Foetal liver, adult spleen and LN cells suspensions were obtained using 70μm strainers. Lineage (Lin) was: Ter119, TCRβ, CD3ε, CD19, NK1.1, CD11c and Gr1. Flow cytometry analysis and cell sorting were performed using FORTESSA, FACSCanto I, FACSAria I and II flow cytometers (BD Biosciences), MoFlo XDP or Cyan ADP flow cytometer (Beckman Coulter). Data analysis was done using FlowJo software (Tristar). Sorted populations were >95% pure.

Cell culture and viral transduction

For *in vitro* stimulation, LN embryonic cells were harvested as previously described[10]. Tissues were digested with Blenzyme 2 (0.5mg/ml, Roche), DNaseI (0.2mg/ml, Roche) in PBS for 15 minutes at 37°C while constant stirring. Cell suspensions were washed with RPMI (Invitrogen), supplemented with 2% heat-inactivated FCS, 100U/ml penicillin, and 100μg/ml streptomycin. For retinoic acid stimulation experiments, *all-trans* retinoic acid ((Sigma-Aldrich) dissolved at 10mM in 100% ethanol) was added at 100nM as previously described[10]. After 24 hours incubation at 37°C and 5% CO_2, cells were isolated and analysed by flow cytometry and RT-PCR. Efficiency of RA treatment was assesses by expression of the RA target gene *Rarb*[16].

Digoxin (Sigma-Aldrich) was dissolved in ethanol at 10mM and used at 10μM, as previously described[40]. Efficiency of digoxin treatment was assessed by expression of the RORγt target genes *Il1r1*, *Il17a*, *Il23r*, *Ccr6*, *Ccl20* and *Csf2*[40].

For treatment of ILC_{4neg} cells *in vitro*, guts and lymph nodes from E15.5 embryos were harvested, digested with collagenase D (5mg/ml; Roche) and DNaseI (0.1mg/ml; Roche) in DMEM, 3% FBS, for approximately 40 minutes at 37°C with gentle agitation. Total cell suspension or flow cytometry sorted cells were starved overnight and stimulated with *all-trans* retinoic acid (Sigma-Aldrich, 1μM) or vehicle (DMSO, 0.0015%, Sigma-Aldrich) for 24 hours at 37°C and 5% CO_2. Cells were analysed by flow cytometry or quantitative real time RT-PCR. For cell culture, ILC_{4neg} cells were sorted from E15.5 guts and lymph nodes and suspended in culture medium OPTI MEM (Invitrogen) supplemented with 20% FBS, penicillin and streptomycin (respectively 50U and 50mg/ml, Invitrogen), sodium pyruvate (1mM, Invitrogen) and β-mercaptoethanol (50mM, Invitrogen) and recombinant murine RANK Ligand (rRANKL; 50ng/ml; Peprotech). Cells were seeded into flat bottom 96-well plates previously coated with 3,000 rad-irradiated OP9 stromal cells for 6 days. E15.5 ILC_{4neg} cells from RAR dominant negative and WT littermate controls were sorted and transduced with pMig.IRES-GFP retroviral empty vector or containing *Rorgt* in the presence of polybrene (0.8mg/mL; Sigma-Aldrich). pMig.IRES-*Rorgt* was a gift of Dr. Littman (Addgene plasmid #24069). Transduced cells were cultured for 6 days. Cultured cells were trypsinised and directly analysed by flow cytometry or FACS sorted and analysed by RT-PCR.

Quantitative RT-PCR

Total RNA was extracted using RNeasy Micro kit (Qiagen) or using Trizol (Invitrogen) according to manufacturer's protocol. RNA concentration was determined using Nanodrop Spectrophotometer (Nanodrop Technologies). Quantitative real time RT-PCR was performed as previously described[6,7,10]. Listed primers are sense and anti-sense, respectively. When a nested-sense primer was used, this is last in the list. Gene sequences were obtained from https://www.ensembl.org. *Rara*: 5′-GCATCCAGAAGAACATGGTG-3′ and 5′-CTCGTTGTTCTGAGCTGTTG-3′; *Rarb*: 5′-AGCCCACCATCTCCACTTC-3′ and 5′-CTCGATGGCAAGTGTAGATC-3′; *Rarg*: 5′-TGCAATGACAAGTCTTCTGG-3′ and : 5′-GTTTTTGTCACGGTGACATG-3′; *Rxra*: 5′-TTCTCTACCCAGGTGAACTC-3′ and 5′-AGGAGGCCATATTTCCTGAG-3′; *Rxrb*: 5′-CAAAGACTGTACAGTGGAC-3′ and 5′-CCTTGGTCACTCTTCTGCTC-3′; *Rxrg*: 5′-TCTTGGCTCTCCGTATAGAG-3′ and 5′-CTGCTGACACTGTTGACCAC-3′; *Hprt1*: 5′-TCCCTGGTTAAGCAGTACAG-3′, 5′-GCTTTGTATTTGGCTTTTCC-3′ and 5′-GACCTCTCGAAGTGTTGGAT-3′.

TaqMan specific primers and probes were from Applied Biosystems. TaqMan Gene Expression Assays were the following: *Gapdh* Mm99999915_g1; *Hprt1* Mm00446968_m1; *Id2* Mm00711781_m1; *Runx1* Mm01213405_m1; *Lta* Mm00440228_gH; *Trance* Mm00441906_m1; *Cxcl10* Mm00445235_m1; *Cxcr5* Mm00432086_m1; *Ccr6* Mm99999114_s1; *Cxcl3* Mm01701838_m1; *Tnfa* Mm00443260_g1; *Cxcl1* Mm04207460_m1; *Nfkbiz* Mm00600522_m1; *Cxcl2* Mm00436450_m1; *Klf4* Mm00516104_m1; *Tox* Mm00455231_m1; *Il22* Mm01226722_g1; *Il17a* Mm00439618_m1; *Il23r* Mm00519943_m1; *Rorc* Mm01261022_m1; *Ltb* Mm00434774_g1; *Notch1* Mm00435249_m1; *Il1r1* Mm00434237_m1, *Ccl20* Mm01268754_m1 and *Csf2* Mm01290062_m1. Gene expression was normalised to *Hprt1*

and *Gapdh*. Real time PCR analysis was performed using ABI Prism 7900HT Sequence Detection System or StepOne Real-Time PCR system (Applied Biosystems).

Bioinformatics and chromatin immunoprecipitation (ChIP) assay

TESS (www.cbil.upenn.edu/tess) web-based-tool was used to identify putative RA response elements (RARE) in the mouse *Rorc* locus. Embryonic ILC_{4neg} cells (2×10^5) were isolated by flow cytometry from E15.5 intestines and PLNs. Cell suspensions were starved overnight and incubated with *all-trans* RA (1μM) or DMSO (0.0015%) for eight hours and fixed with 0.8% formaldehyde (EMS sciences). Cells were lysed and chromosomal DNA-protein complex sonicated to generate DNA fragments ranging from 100–300 bp. DNA/protein complexes were immunoprecipitated using 6μg of rabbit polyclonal antibody against mouse pan-RAR (M-454, Santa Cruz Biotech, Inc), 4μg of rabbit polyclonal antibody against mouse pan-RXR (ΔN197, Santa Cruz Biotech, Inc) or rabbit control IgG (Abcam). Immunoprecipitates were uncross-linked and analysed by quantitative PCR using primer pairs flanking putative RARE sites: A, F-TGAAGCAGCTAGTCACTTCC and R-CAGCTCTCCAGCTTGTATTG; B, F-GAAACTTTATCTGGGGCTGG and R-TGAACTCAGGAAGAGCAGCA; C, F-AACCTGGCACTTCGCACTTAA and R-GAGTGGGCGGACTTCTCAGA; D, F-GAGGCCTCTAAGTACCGCCATT and R-CGCCCTGAATCCTGTCACA; E, F-CAGAGATGACCTAGTCAGTGGAGTACTG and R-ACCCCCCAAAACCCTTGA; F, F-ACCACTGAGCCATCTCTCCTACC and R-TTTTGTGATGTGGGTTCTGGG; G, F-GACAATCTCATCAGAGGAGG and R-GGGCAACCAATGAGTATGTG. Results were normalised to input, intensity and control IgG.

Luciferase reporter assay

Putative RARE sequences were cloned into pTA-Luc firefly Luciferase reporter plasmid (Clontech). Corresponding scrambled mutated sequences were also cloned into the same plasmid. Sequences were cloned in tandems (4 copies). WT and scrambled sequences (1 copy) were, respectively: **C**:
AACCTGGCACTTCGCACTTAAACCTGTGAACTCTGAGAAGTCCGCCCACTC and
AACCTGGCACTTCGCACTTAAACCTGACGTTACTGAGAAGTCCGCCCACTCE; **E**:
CAGAGATGACCTAGTCAGTGGAGTACTGCCACAAACACACTGGGGTCAAGGGTTTTGGGGGGT and
CAGAGACACTTGAGTCAGTGGAGTACTGCCACAAACACACTAGGTGGCGGTAGTTTGGGGGGT; **G**:
GACAATCTCATCAGAGGAGGTCACCTCTACTCTTCCATCACATACTCATTGGTTGCCC and
GACAATCTCATCAGAGGCCTAGTGACACTCTCTTCCATCACATACTCATTGGTTGCCC. Putative binding sites and respective scrambled sequences are underlined. To test the activity of these elements 293T cells were transfected with the aforementioned reporter constructs together with expression vectors expressing murine RARα, RXRα (kind gift from Drs. Vilhais-Neto and Pourquié) and *Renilla*-Luciferase using X-tremeGene9 DNA Transfection Reagent (Roche). At 48 hours cells were starved and 20 hours later treated with DMSO or RA (1μM) for 24 hours, and Luciferase activity was measured in total cell lysates using the Dual-Luciferase Reporter Assay System (Promega). Data were normalised for

transfection efficiency using the ratio between firefly Luciferase activity and *Renilla* Luciferase.

Murid herpesvirus-4 infection

Chimeric mice obtained from transplantation of WT bone marrow (CD45.1) into lethally irradiated RAR^{Het} ($WT \rightarrow Rar^{Het}$) or WT ($WT \rightarrow WT$) littermate control hosts (CD45.2) were used. Mice were infected intranasally with 10^4 PFU of Murid herpesvirus-4 (MuHV-4)[41,42] under isofluorane anaesthesia 12 weeks post transplantation. Intrathoracic lymph nodes and lungs were removed for analysis. Titres of lytic (infectious) virus were determined by plaque assay of freeze-thawed lung tissue homogenates on BHK-21 cells. Plates were incubated for 4 days, then fixed with 4% formal saline and counterstained with toluidine blue for plaque counting. Frequency and number of virus specific CD8 T cells (Tetramer positive) for two viral epitopes (ORF61 and ORF75c) were determined in the draining intrathoracic LNs by tetramer staining (a kind gift from Dr. Ploegh) and flow cytometry[25].

OT1 CD8 T cell activation

Dendritic cells were isolated from single cell suspensions of lymph nodes and spleen from $WT \rightarrow Rar^{Het}$ or $WT \rightarrow WT$ chimeric mice. Cells were negatively depleted for TCRβ, CD19, TER119, Mac1, Gr1, CD3ε using DynaBeads Biotin Binder kit (Life Technologies) and positively enriched for CD11c using MACS Cell Separation Reagents (Miltenyi Biotech). OT1 CD8 T cells were isolated from peripheral lymph nodes of *OT1* Tg $Rag1^{-/-}$ mice by Thy1.2 positive enrichment using MACS Cell Separation Reagents (Miltenyi Biotech). 2.5×10^4 dendritic cells pre-loaded with 10^{-5}μM OVA peptide (Thermo Scientific) were cultured for 3 days with 1.25×10^5 monoclonal OT1 CD8 T cells labeled with 2μM CFSE (BioLegend). Expansion of OT1 CD8 T cells was measured by CFSE dilution and proliferative index was calculated using FlowJo (TreeStar, Inc). Intracellular INFγ levels were measured by flow cytometry using IC fixation/permeabilisation kit (eBioscience).

Antibody list

Cell suspensions were stained for flow cytometry using: anti-CD45 (30-F11); anti-CD11c (N418); anti-CD127 (IL7Rα; A7R34); anti-Ly-6A/E (Sca1; D7); anti-CD45.1 (A20); anti-CD45.2 (104); anti-CD8α (53-6.7); anti-CD19 (eBio1D3); anti-Thy1.2 (53-2.1); anti-NK1.1 (PK136); anti-CD3ε (eBio500A2), TER119 (TER-119), CD11b (Mi/70), Gr1 (RB6-8C5), NK1.1 (PK136), IFNγ (XMG1.2), isotype for IFNγ (eBRG1), α4β7 (DATK32) and MHCII (M5/114.15.2) antibodies and streptavidin fluorochrome conjugates from eBioscience. Anti-CD4 (GK1.5) and TCRβ (H57-595) antibodies were purchased from Biolegend. Anti-RORγt (Q31-378) and RORγt isotype (G155-178) were purchased from BD Pharmingen. Anti-GFP (A11008) antibody was purchased from Invitrogen. Intracellular staining for flow cytometry was performed using IC fixation/permeabilisation kit (eBioscience). Embryo sections for immunofluorescence analysis were stained with GK1.5 (anti-CD4), MP33 (anti-CD45) and A7R34 (anti-IL7Rα; kindly provided by Dr. Nishikawa) purified from hybridoma cell culture supernatants with protein G-Sepharose (Pharmacia). Anti-Ki67 and anti-podoplanin (8.1.1) antidodies were purchased from BD Biosciences and Biolegend, respectively. Embryos were whole mount stained using Alexa Fluor 647-conjugated anti-CD4 (YTS191.1) from AbDSerotec; Intestines were whole mount stained using rat anti-CD106

(VCAM-1, 429 MVCAM.A) from BD Biosciences. Adult LN sections were stained using rabbit polyclonal anti-desmin and rat monoclonal anti-B220 (RA3-6B2) from Abcam and eBioscience, respectively. Anti-species specific Alexa Fluor 594; Alexa Fluor 555; Alexa Fluor 488 or Alexa Fluor 647 were used as secondary antibodies (Invitrogen).

Statistics

Variance was analysed using F-test. Student's *t*-test was performed on homoscedastic populations and student t-test with Welch correction was applied on samples with different variances.

Extended Data

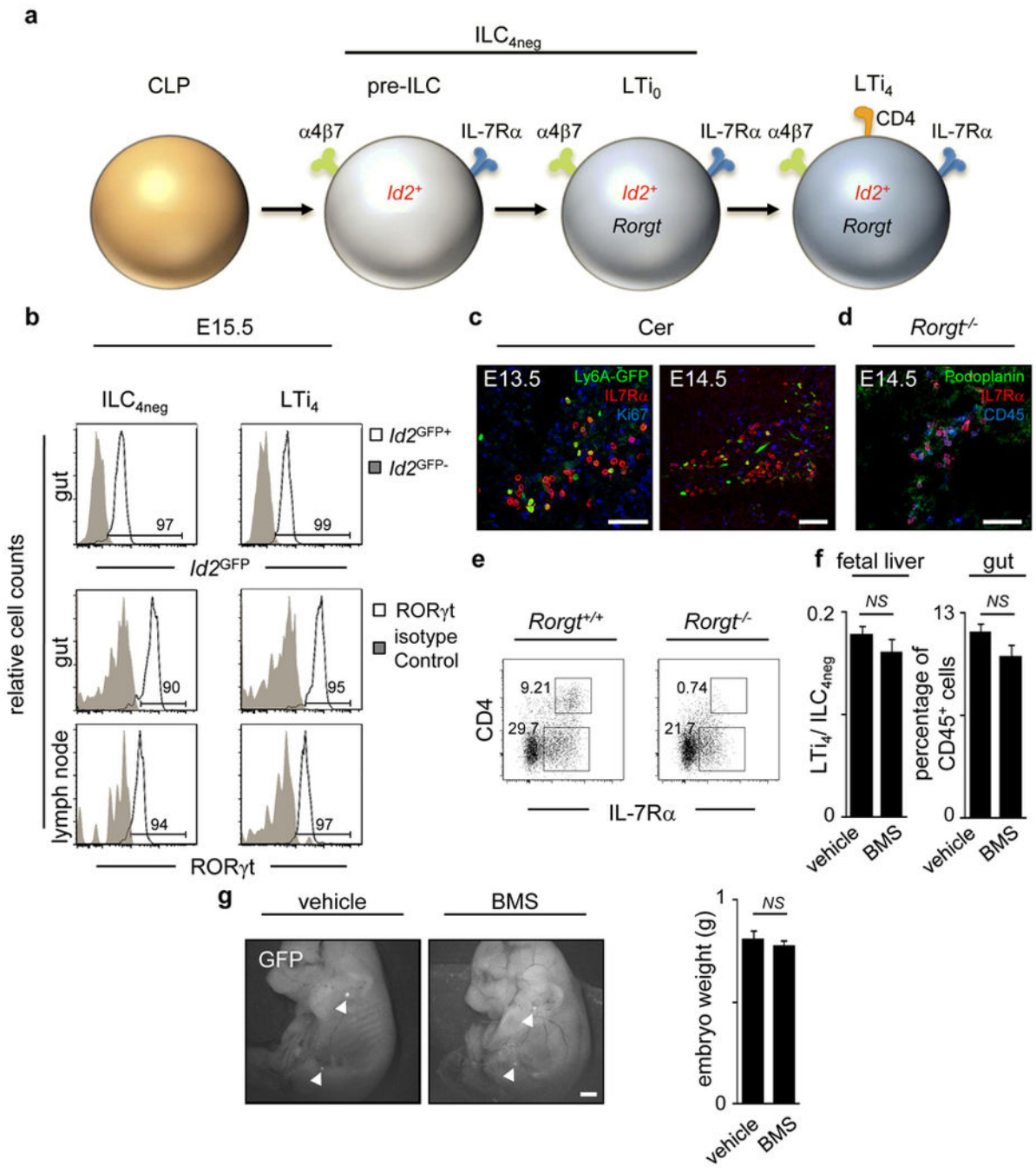

Extended Data Figure 1. Foetal ILCs

a, ILC subsets in foetal gut and LNs. **b**, E15.5 intestines and LN cells were purified from *Id2*^{GFP} and WT mice. *Id2*^{GFP} and RORγt expression are shown in ILC_{4neg} ($CD3^{-}IL7R\alpha^{+}\alpha4\beta7^{+}ID2^{+}$c-$Kit^{+}CD11c^{-}CD4^{-}$) and LTi_4 ($CD3^{-}IL7R\alpha^{+}\alpha4\beta7^{+}ID2^{+}$c-$Kit^{+}CD11c^{-}ROR\gamma t^{+}CD4^{+}$) cells. **c**, E13.5 and E14.5 Ly6A-GFP anlagen LN were stained with GFP, IL7Rα and Ki67 antibodies and analysed by confocal microscopy. **d**, E14.5

Rorgt$^{-/-}$ mesenteric LNs were stained with podoplanin, IL7Rα and CD45 antibodies and analysed by confocal microscopy. **e**, Percentage of E16.5 ILC_{4neg} and LTi_4 cells gated in $CD45^+CD3^-CD11c^-$ determined by flow cytometry in *Rorgt*$^{+/+}$ and *Rorgt*$^{-/-}$ intestines. Data are representative of three independent experiments. **f**, Left: Pregnant mice received RAR antagonist BMS493 or the vehicle DMSO from E10.5 until E13.5. The ratio LTi_4/ILC_{4neg} cells in the foetal liver was determined at E13.5; n=8. Right: Pregnant mice received BMS493 or the vehicle DMSO. Frequency of colonising haematopoietic cells was determined in E17.5 intestines by flow cytometry; n=4. **g**, Pregnant *hCD2*-GFP mice were administered BMS493 or DMSO from E10.5 until E13.5. Embryos were analysed at E17.5; n=13. Arrowheads show anlagen LNs. Scale bars: 50μm (**c**,**d**); 500μm (**g**). Error bars show s.e.. Two tailed t-test p values are indicated. *P<0.05; **P<0.01; ***P<0.001. *n.s.*, not significant.

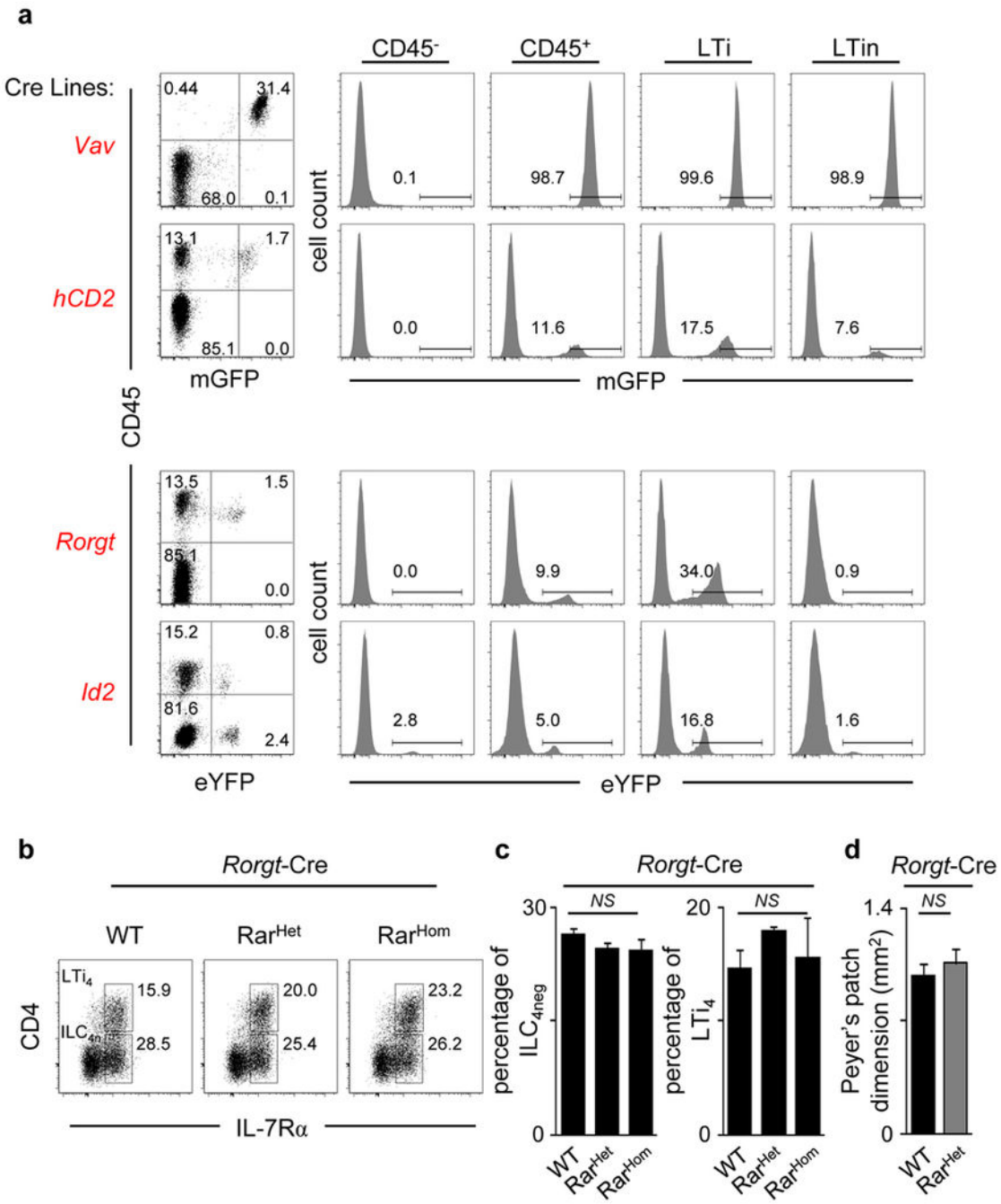

Extended Data Figure 2. Analysis of haematopoietic cell Cre mouse lines

a, *Vav*-iCre and *hCD2*-Cre mice were crossed with *ROSA26*-Tomato-mGFP mice. *Rorgt*-Cre and *Id2*-CreERT2 mice were crossed with *ROSA26*-eYFP mice. E15.5 intestines were analysed by flow cytometry. Left: Results show the percentage of mGFP or eYFP positive cells in gut cell suspensions. Right: Percentage of mGFP or eYFP positive cells in non-haematopoietic ($CD45^{-}$), haematopoietic ($CD45^{+}$), LTi and LTin cells. Results are representative of three independent experiments. **b**, Percentage of enteric E15.5 pre-LTi and LTi_4 cells determined by flow cytometry in WT, *Rorgt*-Cre Rar^{Het} and *Rorgt*-Cre Rar^{Hom}

littermates. **c**, Frequencies of enteric ILC_{4neg} and LTi_4 cells in WT, *Rorgt*-Cre Rar^{Het} and *Rorgt*-Cre Rar^{Hom} littermates. WT n=5; *Rorgt*-Cre Rar^{Het} n= 5; *Rorgt*-Cre Rar^{Hom} n=4. **d**, PP area at 6–7 weeks of age. WT n=3; *Rorgt*-Cre Rar^{Het} n= 4. Two tailed t-test p values are indicated. *P<0.05; **P<0.01; ***P<0.001. *n.s.*, not significant.

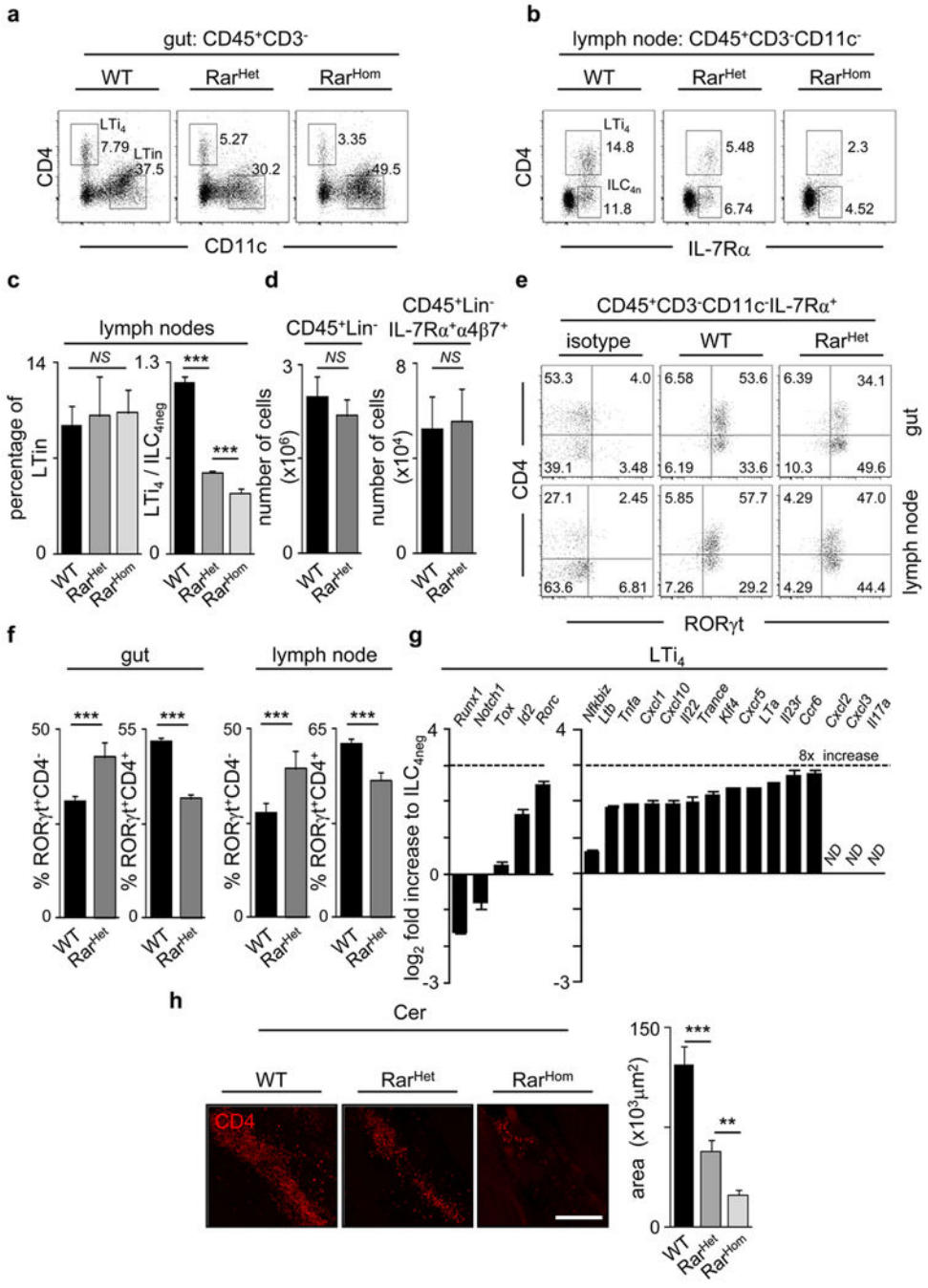

Extended Data Figure 3. Analysis of *Vav*-iCre/*ROSA26*-RARα403 mice

a, E15.5 intestines from WT, *Vav*-iCre Rar^{Het} and Rar^{Hom} mice were analysed by flow cytometry. Representative analysis of six independent experiments is shown. **b**, E15.5

regions of cervical, brachial and inguinal LN from WT, *Vav*-iCre Rar^{Het} and Rar^{Hom} mice were analysed by flow cytometry. Representative analysis of two independent experiments. **c**, LTin cell percentage and LTi_4/ILC_{4neg} cell ratios are shown in E15.5 LNs; n=4. **d**, E15.5 foetal livers from WT and *Vav*-iCre Rar^{Het} mice were analysed by flow cytometry. Results show number of $CD45^+Lin^-$ (n=4) and $CD45^-Lin^-IL7R\alpha^+\alpha4\beta7^+$ progenitors (n=3). **e**, Percentage of $CD45^+CD3^-CD11c^-IL7R\alpha^+ROR\gamma t^+CD4^-$ ($ROR\gamma t^+CD4^-$) and $CD45^+CD3^-CD11c^-IL7R\alpha^+ROR\gamma t^+CD4^+$ ($ROR\gamma t^+CD4^+$) cells determined by flow cytometry in RAR^{Het} and WT littermate controls in E15.5 guts and LNs. **f**, Frequencies of $ROR\gamma t^+CD4^-$ and $ROR\gamma t^+CD4^+$ cells in mice described in (**e**) WT n=9; Rar^{Het} n=3. **g**, ILC_{4neg} cells were purified from E15.5 WT intestines by flow cytometry and cultured for 6 days. LTi_4 cells raised *in vitro* were purified by flow cytometry and quantitative RT-PCR analysis performed. Results show Log_2 fold increase in comparison to their cultured ILC_{4neg} cell counterparts. Results were normalised to *Hprt1* and *Gapdh*. **h.** Left: E15.5 embryos were whole mount stained for CD4 (red) and imaged by confocal microscopy. Cervical (Cer) LNs are shown. Right: Cervical LN dimensions are shown. WT n=5; Rar^{Het} n=7; Rar^{Hom} n=6. Scale bar: 50μm. Two tailed t-test p values are indicated. *P<0.05; **P<0.01; ***P<0.001. *n.s.*, not significant.

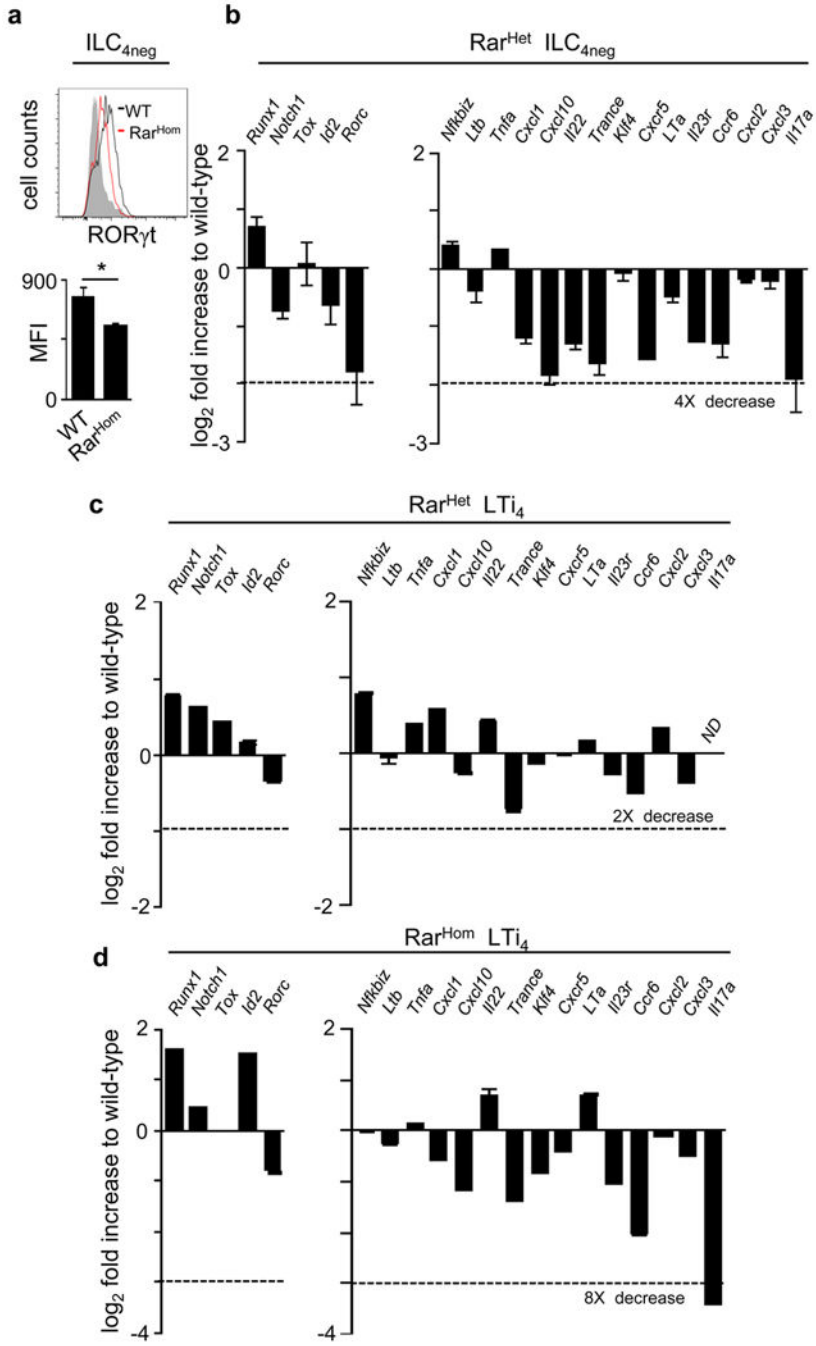

Extended Data Figure 4. Gene expression patterns in ILC$_{4neg}$ and LTi$_4$ cells

a, E15.5 intestines from Rar^{Hom} and WT littermate controls were brought to suspension and analysed by flow cytometry. Upper panel: RORγt expression. Lower panel: mean fluorescence intensity of RORγt expression in ILC$_{4neg}$ cells; n=3. **b**, Pre-LTi cells were purified from E15.5 Rar^{Het} and WT littermate control intestines and lymph nodes. Quantitative RT-PCR analysis was performed. Results show Log$_2$ fold increase to WT. Results were normalised to *Hprt1* and *Gapdh*. Results from three independent measurements are shown. **c**,**d**, LTi$_4$ cells were purified from E15.5 Rar^{Het} (**c**), Rar^{Hom} (**d**) and WT

littermate control intestines and lymph nodes. Quantitative RT-PCR analysis was performed. Results show Log_2 fold increase to WT. Results were normalised to *Hprt1* and *Gapdh*. Data from three independent measurements are shown. Two tailed t-test p values are indicated. *P<0.05; **P<0.01; ***P<0.001. *n.s.*, not significant.

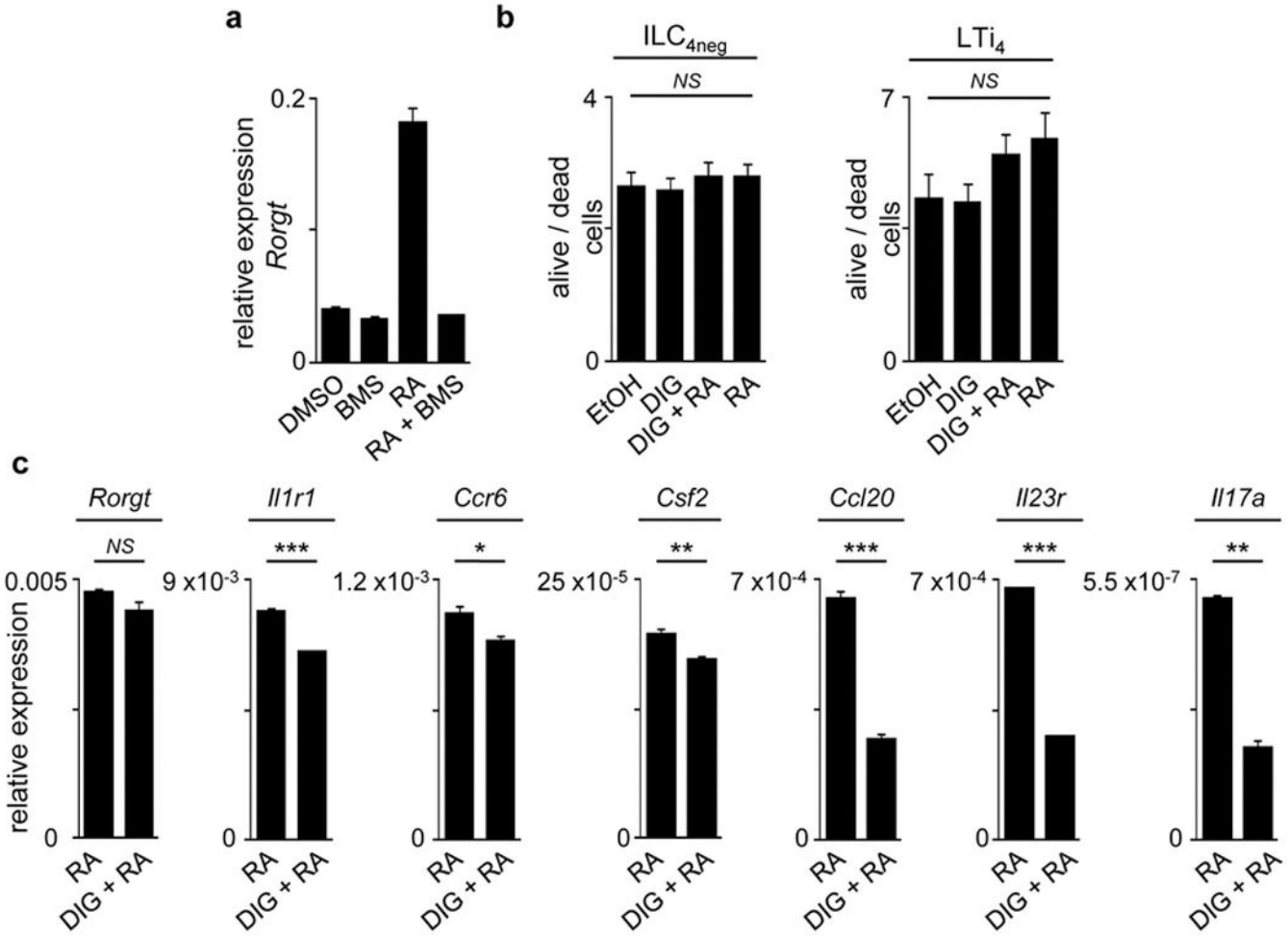

Extended Data Figure 5. Treatment of ILC_{4neg} and LTi_4 cells with digoxin

a, WT ILC_{4neg} cell were FACS purified starved overnight and stimulated with DMSO, BMS493 (100nM), RA (100nM) and RA+BMS493 (100nM each) for 16 hours. Results show quantitative RT-PCR analysis normalised to *Gapdh*; n=3. **b**, E13.5 LN cell suspensions were cultured with vehicle (ethanol), digoxin, digoxin+RA and RA alone for 24H. Alive/dead cell ratios were determined by flow cytometry and DAPI staining; n=4. **c**, ILC_{4neg} cells were isolated from WT E15.5 embryos starved overnight and stimulated for 6 hours in the presence of RA (100nM) or DIG (10μM) + RA (100nM). Results show quantitative RT-PCR analysis of *Rorgt* and RORγt downstream targets normalised to *Gapdh*. Representative of three independent experiments. Error bars show s.e.. Two tailed t-test p values are indicated. *P<0.05; **P<0.01; ***P<0.001. *n.s.*, not significant.

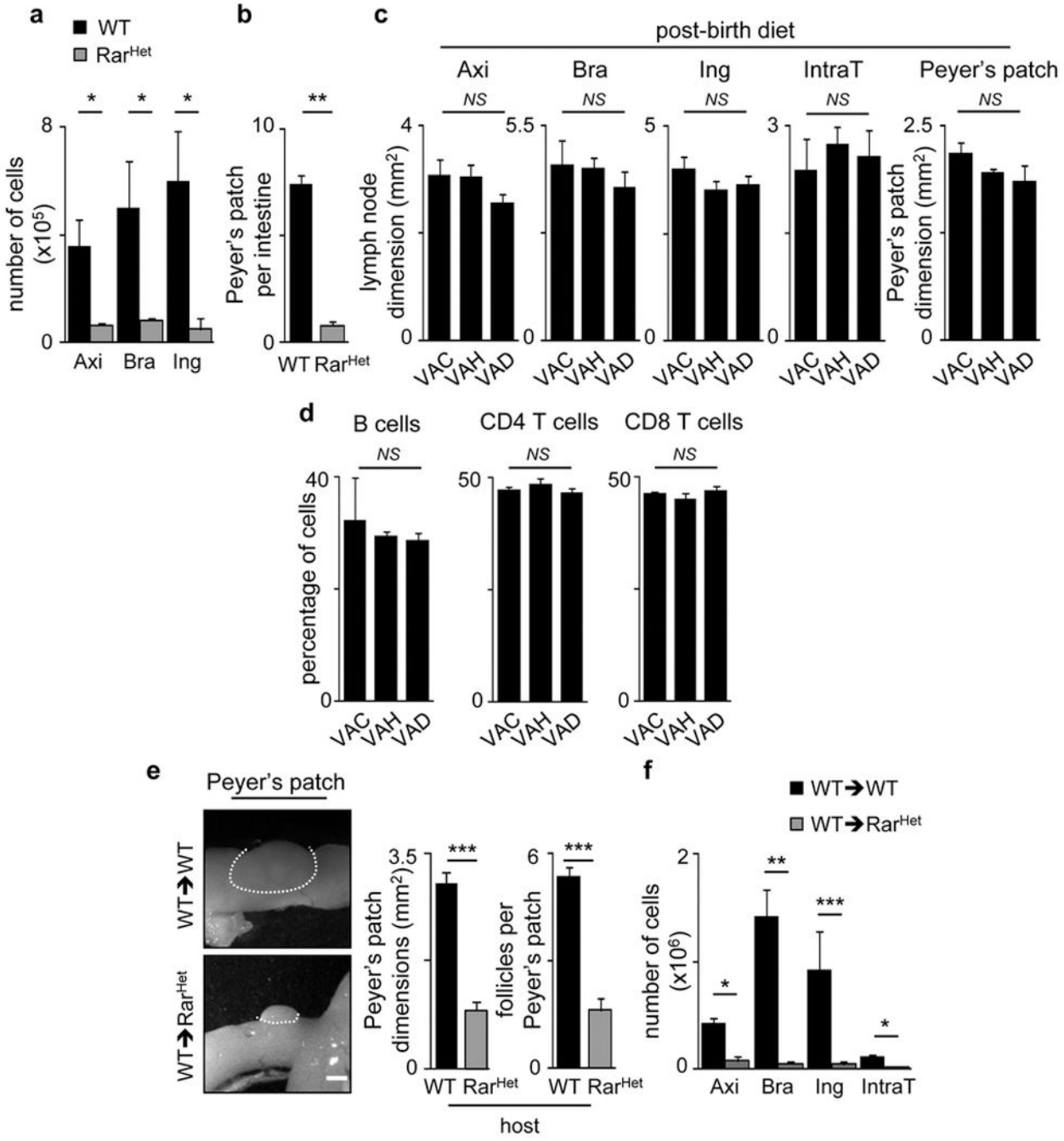

Extended Data Figure 6. Analysis of SLOs from adult mice with variable RA signalling levels

a, Axillary (Axi), brachial (Bra) and inguinal (Ing) LNs from adult Rar^{Het} and WT littermate controls were analysed. Results show LN cell numbers; n=6. **b**, Results show PP number per intestine from adult Rar^{Het} and WT littermate controls; n=6. **c.** Six-week old WT females received VAC, VAH or VAD (n=3) diet for 7 weeks. Axillary (Axi), brachial (Bra), inguinal (Ing), intrathoracic (IntraT) LNs and Peyer's patches (PP) dimensions were analysed; n=3. **d.** Percentage of $CD45^+CD19^+$ B cells; $CD4^+$ and $CD8^+$ T cells in inguinal LNs; n=3. **e**,**f**, Two week-old CD45.2 Rar^{Het} and WT littermate controls were lethally irradiated and

transplanted with WT CD45.1 bone marrow cells. Chimeric mice were analysed 8 weeks after reconstitution. **e**, Results show PP dimensions and follicle number/PP; n=6. **f**, Results show number of cells in axillary (Axi), brachial (Bra) inguinal (Ing) and intrathoracic (Intra T) LNs; n=6. Scale bar: 1mm. Error bars show s.e.. Two tailed t-test p values are indicated. *P<0.05; **P<0.01; ***P<0.001. *n.s.*, not significant.

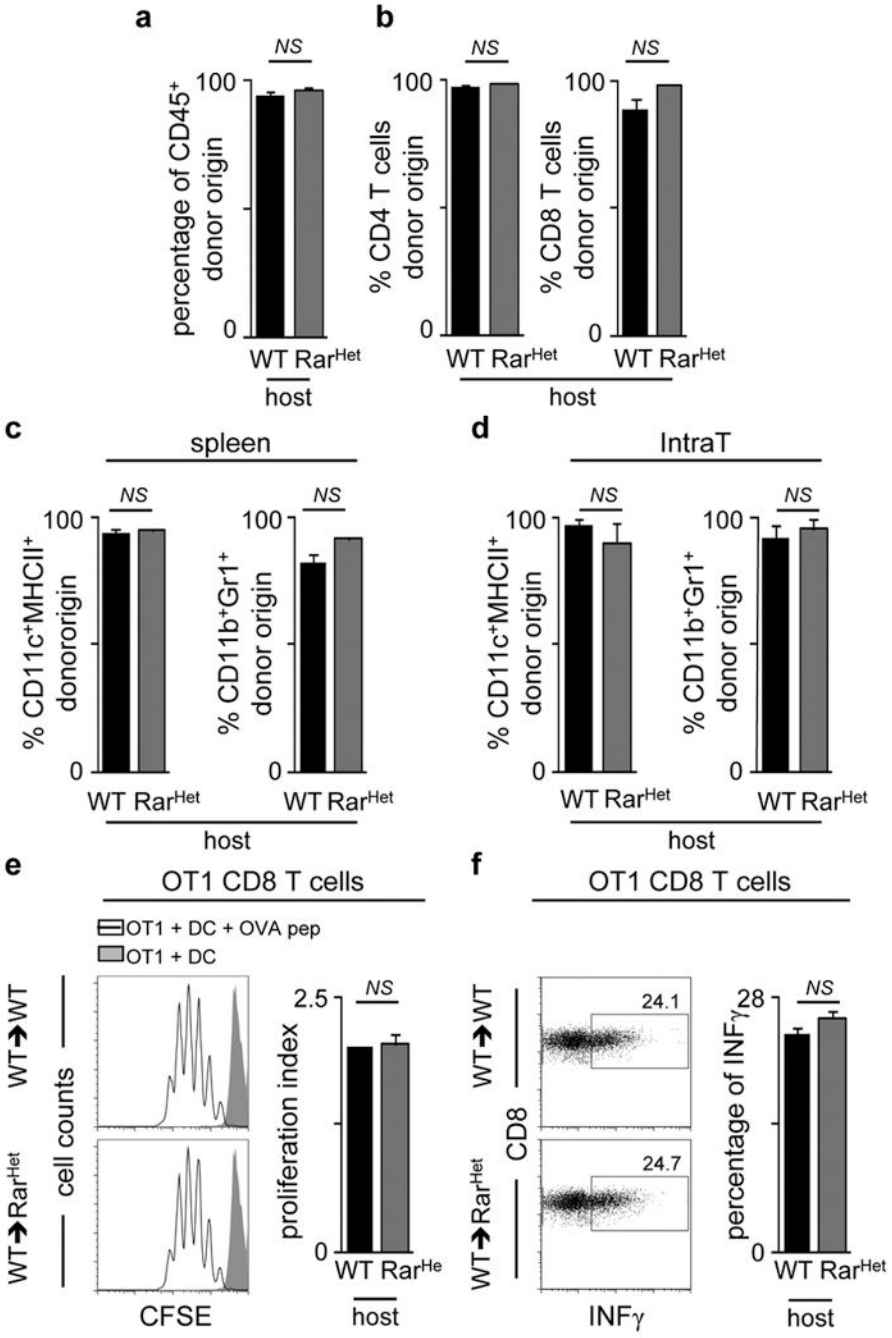

Extended Data Figure 7. Analysis of WT→WT and WT→Rar^{Het} bone marrow chimeras

Two week-old CD45.2 Rar^{Het} and WT littermate controls were lethally irradiated and transplanted with WT CD45.1 bone marrow cells. Chimeric mice were analysed 8 weeks after reconstitution. **a**, Reconstitution of donor CD45.1 cells in WT→WT and WT→Rar^{Het} chimeras in the spleen (n=4). **b**, Reconstitution of donor CD45.1 CD4 and CD8 T cells in WT→WT and WT→Rar^{Het} chimeras in the spleen. WT→WT n=4; WT→Rar^{Het} n=11. **c**, Reconstitution of donor CD45.1 $CD11c^{+}MHCII^{+}$ and $CD11b^{+}Gr1^{+}$ myeloid cells in WT→WT and WT→Rar^{Het} chimeras in the spleen; n=3. **d**, Reconstitution of donor CD45.1 $CD11c^{+}MHCII^{+}$ and $CD11b^{+}Gr1^{+}$ cells in WT→WT and WT→Rar^{Het} chimeras in intrathoracic LNs; n=3. **e**, Dendritic cells (DCs) were purified from WT→WT and WT→Rar^{Het} chimeras. DCs were loaded with OVA peptide (10^{-5} μM) and co-cultured for 3 days with CFSE-labelled monoclonal OT1 CD8 T cells. OT1 CD8 T cell proliferation was analysed by CFSE dilution. Proliferation index is shown. WT n=4; Rar^{Het} n=6. **f**, Dendritic cells (DCs) were purified from WT→WT and WT→Rar^{Het} chimeras. DCs were loaded with OVA peptide (10^{-5} μM) and co-cultured for 3 days with OT1 CD8 T cells. Percentage of IFNγ producing OT1 CD8 T cells is shown; n=4. Error bars show s.e.. Two tailed t-test p values are indicated. *P<0.05; **P<0.01; ***P<0.001. *n.s.*, not significant.

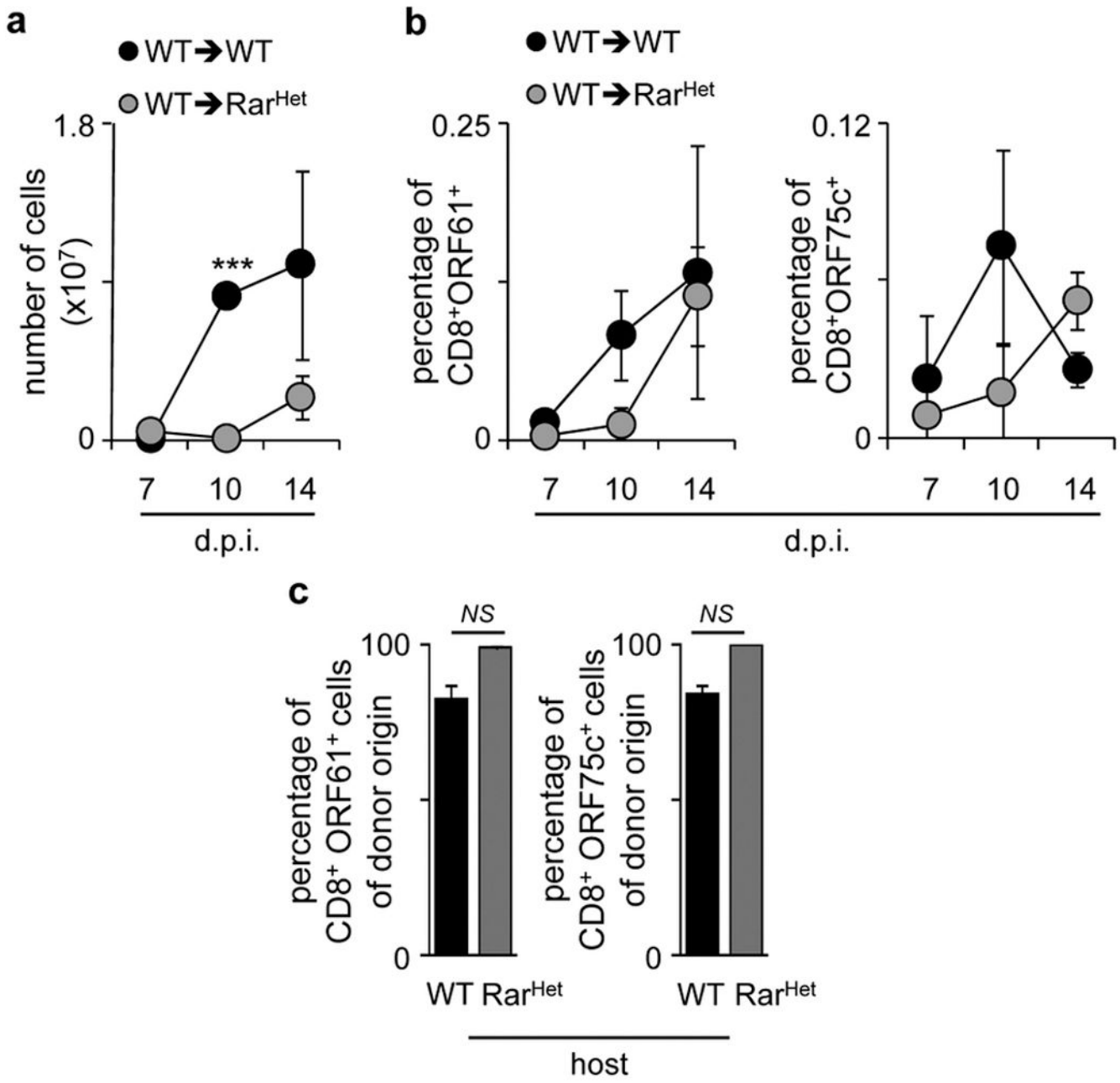

Extended Data Figure 8. Infection of WT→Rar^{Het} or WT→WT chimeras with Murid herpesvirus-4

a, Intrathoracic lymph node cellularity in WT→WT and WT→Rar^{Het} chimeras at different days post infection (dpi). WT n=5; Rar^{Het} n=3. **b**, Percentage of CD8$^+$ORF61$^+$ (left) and ORF75c$^+$ (right) T cells in intrathoracic lymph nodes at different days post infection (dpi). WT n=5; Rar^{Het} n=3. **c**. Percentage of donor CD45.1 CD8$^+$ORF61$^+$ (left) and CD8$^+$ORF75c$^+$ (right) T cells in WT→WT and WT→Rar^{Het} chimeras after infection with Murid herpesvirus-4. WT n=6; Rar^{Het} n=12. Error bars show s.e.. Two tailed t-test p values are indicated. *P<0.05; **P<0.01; ***P<0.001. *n.s.*, not significant.

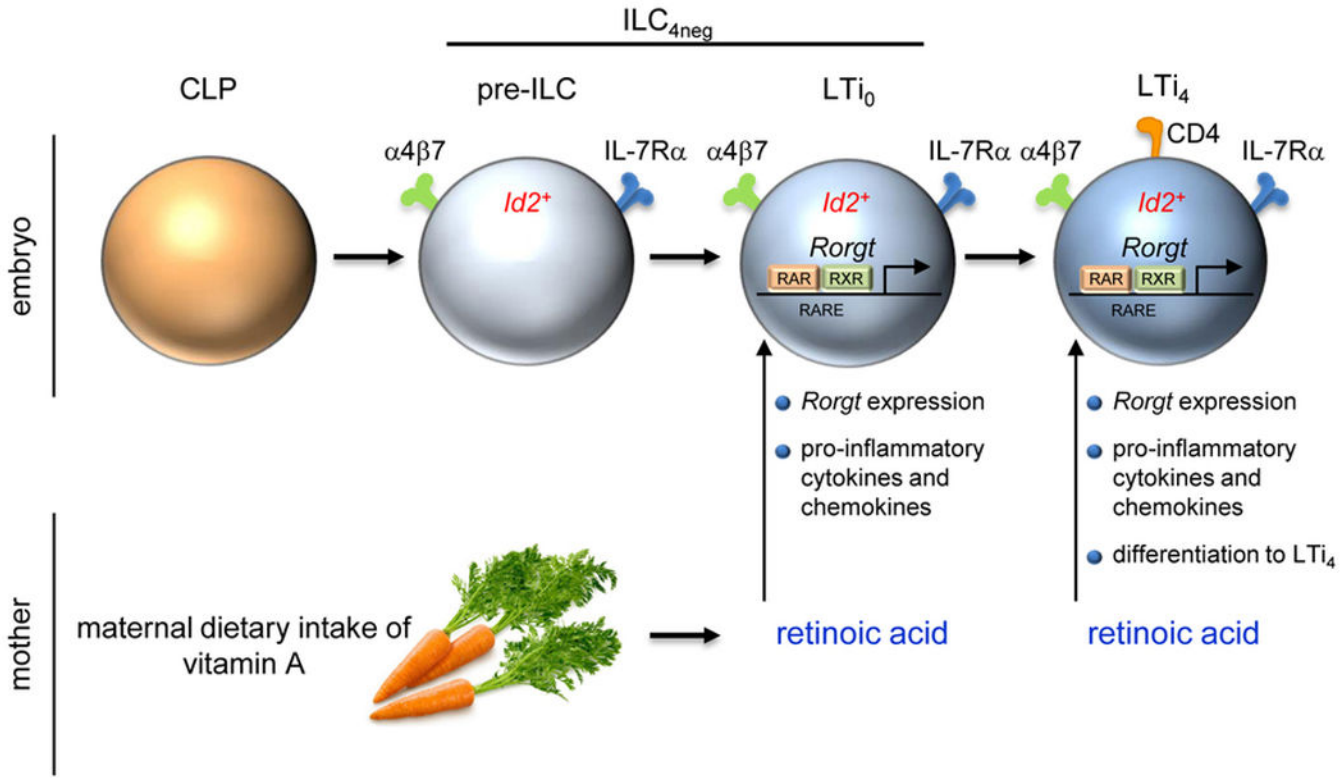

Extended Data Figure 9. Impact of maternal retinoids in ILC3s

Maternal dietary intake of vitamin A is catabolised into bioactive retinoic acid (RA). RA signals control type 3 innate lymphoid cells (ILC3) in the embryo. Foetal ILC3s include ILC_{4neg} and LTi_4 cells. LTi_4 cells are $Id2^+ROR\gamma t^+$, while enteric ILC_{4neg} cells contain a minor subset of $Id2^+ROR\gamma t^-$ cells (pre-ILCs). RA signalling operates in a cell-autonomous fashion, via direct regulation of *Rorgt*, programming innate pro-inflammatory cytokines and chemokines and differentiation of LTi_4 cells.

Extended Data Table 1
Computational analysis of putative RARE sites in the *Rorc* locus

Computational analysis was performed using TESS (Transcription Element Search System) (www.cbil.upenn.edu/tess). TSS (*Rorg*): ACGGGCCAGGTGCTCCCTCC; TSS (*Rorgt*): AGAAACACTGGGGGAGAGCTTTG.

Site ID	Primer Sequences	Putative RARE Sites	Position	TES
A	TGAAGCAGCTAGTCACTTCC CAGCTCTCCAGCTTGTATTG	GAGGAGCAGGG	−7.837 *Rorg* TSS	C
B	GAAACTTTATCTGGGGCTGG TGAACTCAGGAAGAGCAGCA	GGTTCAGAGGT	−7,446 *Rorg* TSS	G
C	AACCTGGCACTTCGCACTTAA GAGTGGGCGGACTTCTCAGA0	TGAACT	−5.478 *Rorg* TSS	
D	GAGGCCTCTAAGTACCGCCATT CGCCCTGAATCCTGTCACA	AGGTCAGCACCA	−4.690 *Rorg* TSS	

Site ID	Primer Sequences	Putative RARE Sites	Position	TES
				AC
E	CAGAGATGACCTAGTCAGTGGAGTACTG ACCCCCCAAAACCCTTGA	GGGGTCAAGGGT TGACCT	−1,800 *Rorg* TSS	G
F	ACCACTGAGCCATCTCTCCTACC TTTTGTGATGTGGGTTCTGGG	GGGTCA	−1,638 *Rorg* TSS	
G	GACAATCTCATCAGAGGAGG GGGCAACCAATGAGTATGTG	TCACCTCT	−1.619 *Rorgt* TSS	

Acknowledgments

We thank the imaging, animal and flow cytometry facilities at IMM and UPC for technical assistance; Cathy Mendelsohn for proving *ROSA26*-RARa403 mice; N. Schmolka, J.G. van Rietschoten, R.E. van Kesteren, T.H.B. Geijtenbeek, S. Gringhuis, E. Keuning, J. Peterson-Maduro, M.G. Roukens, D. D'Astolfo, M. Vermunt, A.Rijerkerk, J. Koning, J. van der Meulen and B. Oliver for technical help; G. Vilhais-Neto, M.C. Coles, G. Eberl for helpful discussion. M. F., L. M.-S. and R. G. D. were supported by FCT, Portugal; H.V.-F. by EMBO (1648) and ERC (207057); D.R.L. by NIH (RO1AI080885) and HHMI; M.R.M. by Dutch MS research foundation (MS 12–797); S.A.vd.P. by NGI Breakthrough Horizon (40-41009-98-9077); and R.E.M. by a VICI (918.56.612) and ALW-TOP grant (09.048).

References

1. Gluckman PD, Hanson MA. Living with the past: evolution, development, and patterns of disease. Science. 2004; 305:1733–1736. [PubMed: 15375258]
2. van de Pavert SA, Mebius RE. New insights into the development of lymphoid tissues. Nat Rev Immunol. 2010; 10:664–674. [PubMed: 20706277]
3. Randall TD, Carragher DM, Rangel-Moreno J. Development of secondary lymphoid organs. Annu Rev Immunol. 2008; 26:627–650. [PubMed: 18370924]
4. Mebius RE, Rennert P, Weissman IL. Developing lymph nodes collect CD4+CD3- LTbeta+ cells that can differentiate to APC, NK cells, and follicular cells but not T or B cells. Immunity. 1997; 7:493–504. [PubMed: 9354470]

5. Eberl G, et al. An essential function for the nuclear receptor RORgamma(t) in the generation of fetal lymphoid tissue inducer cells. Nat Immunol. 2004; 5:64–73. [PubMed: 14691482]
6. Veiga-Fernandes H, et al. Tyrosine kinase receptor RET is a key regulator of Peyer's Patch organogenesis. Nature. 2007; 446:547–551. [PubMed: 17322904]
7. Patel A, et al. Differential RET signaling pathways drive development of the enteric lymphoid and nervous systems. Sci Signal. 2012; 5:ra55. [PubMed: 22855506]
8. Cupedo T, et al. Presumptive lymph node organizers are differentially represented in developing mesenteric and peripheral nodes. J Immunol. 2004; 173:2968–2975. [PubMed: 15322155]
9. Cherrier M, Sawa S, Eberl G. Notch, Id2, and RORgammat sequentially orchestrate the fetal development of lymphoid tissue inducer cells. J Exp Med. 2012; 209:729–740. [PubMed: 22430492]
10. van de Pavert SA, et al. Chemokine CXCL13 is essential for lymph node initiation and is induced by retinoic acid and neuronal stimulation. Nat Immunol. 2009; 10:1193–1199. [PubMed: 19783990]
11. Niederreither K, Dolle P. Retinoic acid in development: towards an integrated view. Nat Rev Genet. 2008; 9:541–553. [PubMed: 18542081]
12. Iwata M. Retinoic acid production by intestinal dendritic cells and its role in T-cell trafficking. Semin Immunol. 2009; 21:8–13. [PubMed: 18849172]
13. Hall JA, et al. Essential role for retinoic acid in the promotion of CD4(+) T cell effector responses via retinoic acid receptor alpha. Immunity. 2011; 34:435–447. [PubMed: 21419664]
14. Mora JR, von Andrian UH. Role of retinoic acid in the imprinting of gut-homing IgA-secreting cells. Semin Immunol. 2009; 21:28–35. [PubMed: 18804386]
15. Mucida D, et al. Retinoic acid can directly promote TGF-beta-mediated Foxp3(+) Treg cell conversion of naive T cells. Immunity. 2009; 30:471–472. author reply 472–473. [PubMed: 19371709]
16. Hall JA, Grainger JR, Spencer SP, Belkaid Y. The role of retinoic acid in tolerance and immunity. Immunity. 2011; 35:13–22. [PubMed: 21777796]
17. de Boer J, et al. Transgenic mice with hematopoietic and lymphoid specific expression of Cre. Eur J Immunol. 2003; 33:314–325. [PubMed: 12548562]
18. Rosselot C, et al. Non-cell-autonomous retinoid signaling is crucial for renal development. Development. 2010; 137:283–292. [PubMed: 20040494]
19. Sun Z, et al. Requirement for RORgamma in thymocyte survival and lymphoid organ development. Science. 2000; 288:2369–2373. [PubMed: 10875923]
20. Yokota Y, et al. Development of peripheral lymphoid organs and natural killer cells depends on the helix-loop-helix inhibitor Id2. Nature. 1999; 397:702–706. [PubMed: 10067894]
21. Aliahmad P, de la Torre B, Kaye J. Shared dependence on the DNA-binding factor TOX for the development of lymphoid tissue-inducer cell and NK cell lineages. Nat Immunol. 2010; 11:945–952. [PubMed: 20818394]
22. Possot C, et al. Notch signaling is necessary for adult, but not fetal, development of RORgammat(+) innate lymphoid cells. Nat Immunol. 2011; 12:949–958. [PubMed: 21909092]
23. Tachibana M, et al. Runx1/Cbfbeta2 complexes are required for lymphoid tissue inducer cell differentiation at two developmental stages. J Immunol. 2011; 186:1450–1457. [PubMed: 21178013]
24. Meier D, et al. Ectopic lymphoid-organ development occurs through interleukin 7-mediated enhanced survival of lymphoid-tissue-inducer cells. Immunity. 2007; 26:643–654. [PubMed: 17521585]
25. Gredmark-Russ S, Cheung EJ, Isaacson MK, Ploegh HL, Grotenbreg GM. The CD8 T-cell response against murine gammaherpesvirus 68 is directed toward a broad repertoire of epitopes from both early and late antigens. J Virol. 2008; 82:12205–12212. [PubMed: 18922872]
26. Kiss EA, et al. Natural aryl hydrocarbon receptor ligands control organogenesis of intestinal lymphoid follicles. Science. 2011; 334:1561–1565. [PubMed: 22033518]

27. Lee JS, et al. AHR drives the development of gut ILC22 cells and postnatal lymphoid tissues via pathways dependent on and independent of Notch. Nat Immunol. 2011; 13:144–151. [PubMed: 22101730]
28. Qiu J, et al. The aryl hydrocarbon receptor regulates gut immunity through modulation of innate lymphoid cells. Immunity. 2011; 36:92–104. [PubMed: 22177117]
29. Karrer U, et al. On the key role of secondary lymphoid organs in antiviral immune responses studied in alymphoplastic (aly/aly) and spleenless (Hox11(-)/-) mutant mice. J Exp Med. 1997; 185:2157–2170. [PubMed: 9182687]
30. Spencer SP, et al. Adaptation of innate lymphoid cells to a micronutrient deficiency promotes type 2 barrier immunity. Science. 2014; 343:432–437. [PubMed: 24458645]
31. Rawlins EL, Clark CP, Xue Y, Hogan BL. The Id2+ distal tip lung epithelium contains individual multipotent embryonic progenitor cells. Development. 2009; 136:3741–3745. [PubMed: 19855016]
32. Eberl G, Littman DR. Thymic origin of intestinal alphabeta T cells revealed by fate mapping of RORgammat+ cells. Science. 2004; 305:248–251. [PubMed: 15247480]
33. Srinivas S, et al. Cre reporter strains produced by targeted insertion of EYFP and ECFP into the ROSA26 locus. BMC Dev Biol. 2001; 1:4. [PubMed: 11299042]
34. Muzumdar MD, Tasic B, Miyamichi K, Li L, Luo L. A global double-fluorescent Cre reporter mouse. Genesis. 2007; 45:593–605. [PubMed: 17868096]
35. de Bruijn MF, et al. Hematopoietic stem cells localize to the endothelial cell layer in the midgestation mouse aorta. Immunity. 2002; 16:673–683. [PubMed: 12049719]
36. Hogquist KA, et al. T cell receptor antagonist peptides induce positive selection. Cell. 1994; 76:17–27. [PubMed: 8287475]
37. Mombaerts P, et al. RAG-1-deficient mice have no mature B and T lymphocytes. Cell. 1992; 68:869–877. [PubMed: 1547488]
38. Niederreither K, et al. Embryonic retinoic acid synthesis is essential for heart morphogenesis in the mouse. Development. 2001; 128:1019–1031. [PubMed: 11245568]
39. Veiga-Fernandes H, Foster K, Patel A, Coles M, Kioussis D. Visualisation of lymphoid organ development. Methods Mol Biol. 2010; 616:161–179. [PubMed: 20379875]
40. Huh JR, et al. Digoxin and its derivatives suppress TH17 cell differentiation by antagonizing RORgammat activity. Nature. 2011; 472:486–490. [PubMed: 21441909]
41. Sunil-Chandra NP, Efstathiou S, Arno J, Nash AA. Virological and pathological features of mice infected with murine gamma-herpesvirus 68. J Gen Virol. 1992; 73(Pt 9):2347–2356. [PubMed: 1328491]
42. Weck KE, Barkon ML, Yoo LI, Speck SH, Virgin HI. Mature B cells are required for acute splenic infection, but not for establishment of latency, by murine gammaherpesvirus 68. J Virol. 1996; 70:6775–6780. [PubMed: 8794315]

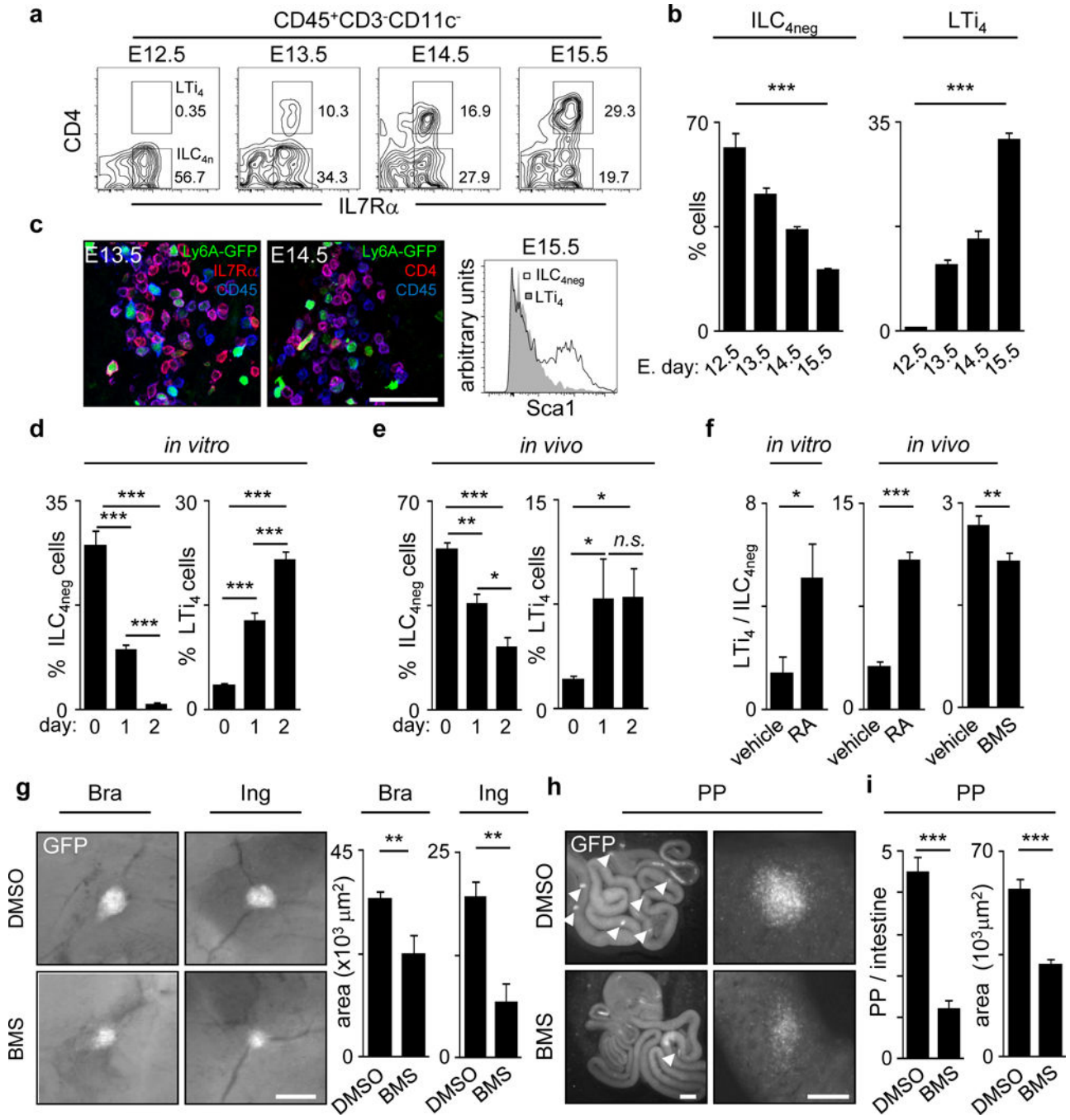

Figure 1. Maternal RA controls LTi differentiation

a, Enteric foetal ILC_{4neg} and LTi_4 cells. **b**, E12.5 n=8; E13.5 n=3; E14.5 n=6; E15.5 n=3. **c**, Left: *Sca1-GFP* LNs. Right: E15.5 gut cells. **d**,**e**, Cultured or transplanted E12.5 guts. **d**, d0 n=4; d1 n=6; d2 n=6. **e**, d0 n=7; d1 n=3; d2 n=5. **f**, Left: E13.5 LN cells; n=7. Centre: RA was provided to females. E13.5 LN cells; n=8. Right: Females received BMS493; n=8. **g–i**, *hCD2-GFP* females received BMS493. E17.5 SLOs. **g**, Brachial and inguinal LNs; n=6. **h**, Arrowheads: PP. **i**, Dimensions; DMSO n=8; BMS n=22. Area; DMSO n=30; BMS n=25.

Scale bar: 50μm (**c**), 200μm (**g**, **h** right), 1mm (**h** left). Error bars show s.e.. *P<0.05; **P<0.01; ***P<0.001.

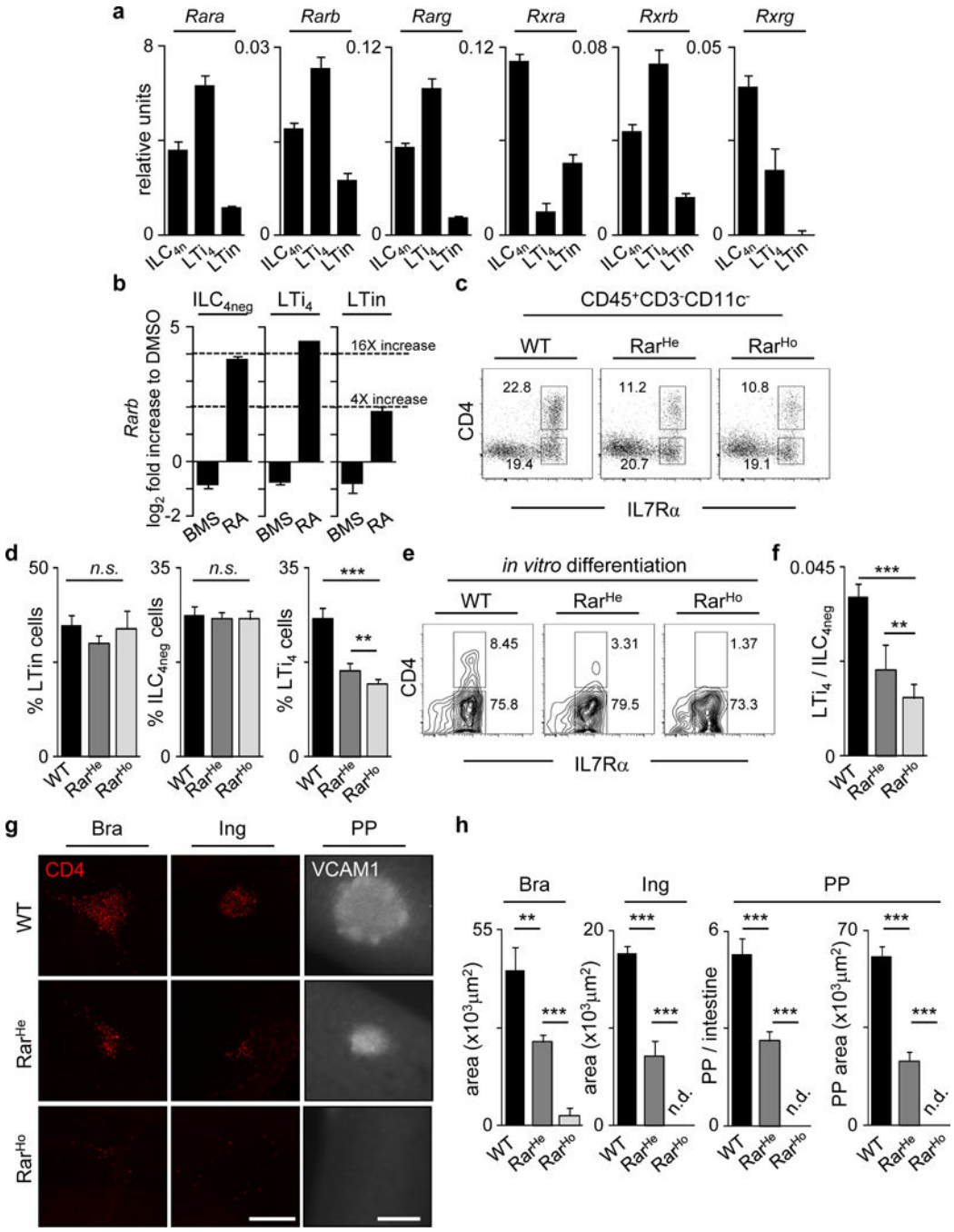

Figure 2. Cell-autonomous RA controls LTi cells and SLO development

a, RT-PCR of enteric cells. Represents 3 independent experiments. **b**, DMSO, BMS493 or RA stimulation. Represents 3 independent experiments. **c**, E15.5. enteric ILC subsets. **d**, LTin n=4. ILC_{4neg} n=5. LTi_4 n=5. **e**, E15.5 ILC_{4neg} cells cultured for 6 days. **f**, ILC_{4neg} cell cultures at day 6; n=5. **g**, E15.5. CD4 (red); VCAM1 (grey). Scale bars: 200µm. **h**, SLO size; n=6. Error bars show s.e.. *P<0.05; **P<0.01; ***P<0.001.

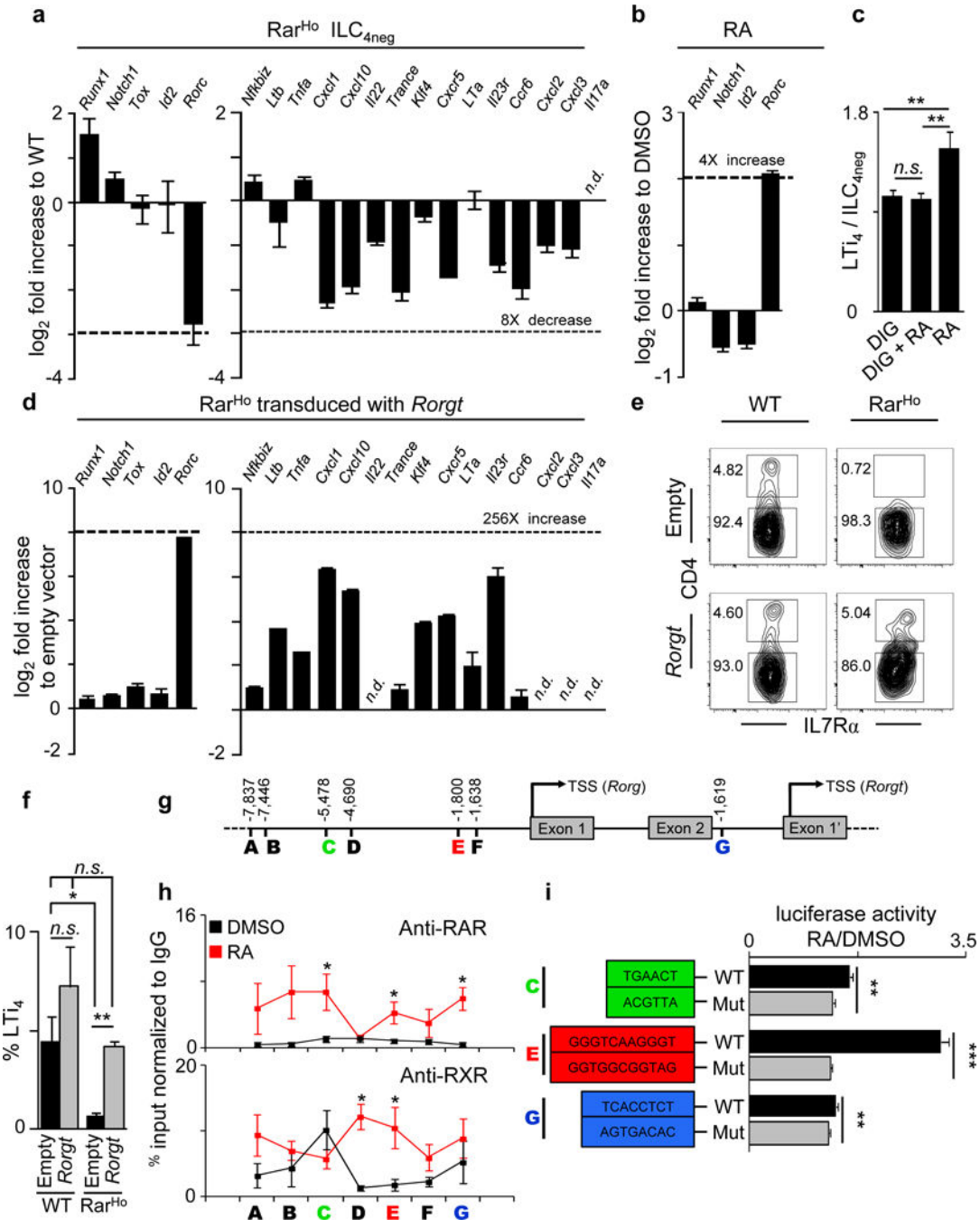

Figure 3. RA controls LTi cells via RORγt

a, E15.5 ILC_{4neg} cells. Represents 3 experiments. **b**, E15.5 ILC_{4neg} cells stimulated with RA. Represents 3 experiments. **c**, E13.5 LN cells stimulated with RA and digoxin; n=16. **d-f**, ILC_{4neg} cells transduced with pMig.*Rorgt*-IRES-GFP virus (day 6). **d**, Represents 3 experiments. **e**, Cytometry analysis. **f**, Emergent LTi_4 cells. WT n=5; Rar^{Ho} n=3. **g**, RARE sites. **h**, E15.5 ILC_{4neg} cells stimulated with RA. ChIP analysis of 5 biological replicates. **i**, Luciferase activity of RARE WT and mutated sites. C n=6; E n=9; G n=6. Error bars show s.e.. *P<0.05; **P<0.01; ***P<0.001. *n.d.*: not detected.

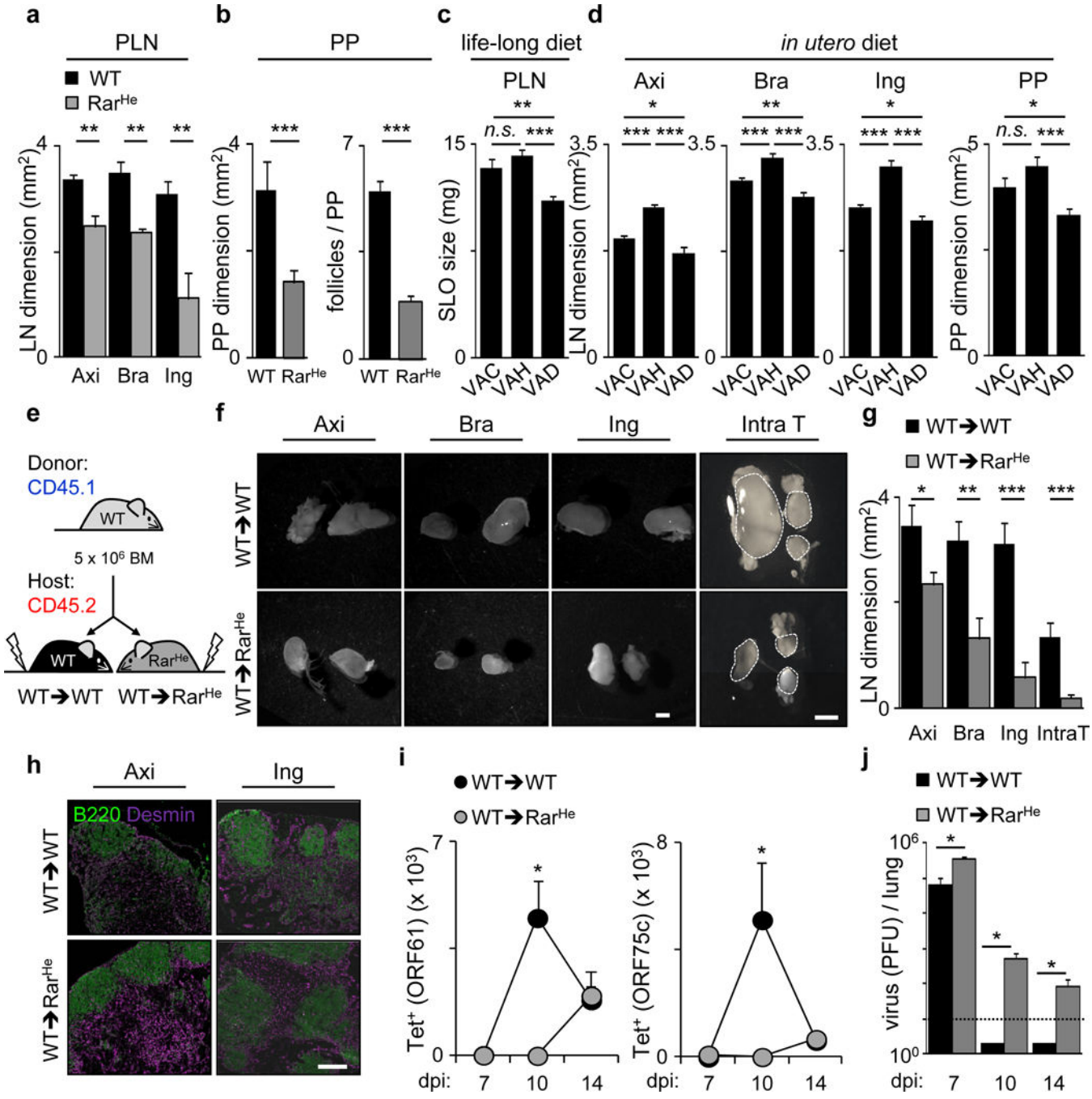

Figure 4. Retinoid levels *in utero* determine the offspring immunity

a, Adult axillary, brachial and inguinal LNs. n=6. **b**, WT n=26; Rar^{He} n=23. **c**, Females received diets that were maintained in the offspring. VAC n=10; VAH n=8; VAD n=18. **d**, Females received variable diets. Their offspring received VAC diet. LN: VAC n=18; VAH n=24; VAD n=25. PP: VAC n=20; VAH n=40; VAD n=63. **e**, Transplantation scheme. **f**, Chimeric LNs. Scale bar: 1mm. **g**, Chimeric LNs. n=6. **h**, Chimeric LNs. Scale bar: 200μm. **i**, Chimeras infected with Murid herpesvirus-4. Tetramer positive CD8 T cells in intrathoracic LNs. **j**, Virus titers (PFU/lung). dpi7: WT→WT n=3; WT→Rar^{Het} n=3. dpi10:

WT→WT n=4; WT→Rar^{Het} n=3. dpi14: WT→WT n=8; WT→Rar^{Het} n=5. Dash line: detection limit. Error bars show s.e.. *P<0.05; **P<0.01; ***P<0.001.